Effects of Constituent Elements and Fabrication Methods on Mechanical Behavior of High-Entropy Alloys: A Review

ZONGYANG LYU, CHANHO LEE, SHAO-YU WANG, XUESONG FAN, JIEN-WEI YEH, and PETER K. LIAW

High-entropy alloys (HEAs) have become a research hotspot in recent years. The nature of the multi-principal elements, high mixing entropy, and mutual interactions between elements render this novel material outstanding mechanical and functional properties, in which most research efforts are focused on mechanical properties. There are many aspects that can influence the mechanical behavior, such as constituent elements and fabrication methods. This paper will mainly summarize and discuss the effects of constituent elements and fabrication techniques on the mechanical properties of HEAs, by reviewing relevant papers, to have a better understanding of the variation ranges resulting from the above two factors and the reasons for the properties changes. Future directions are provided at the end of this article.

https://doi.org/10.1007/s11661-018-4970-z

I. INTRODUCTION

A. *Historical Development of High-Entropy Alloys*

As more new materials are emerging, a novel alloy system has attracted extensive attention in recent years, *i.e.*, high-entropy alloys (HEAs). HEAs, unlike the traditional alloys, which are based on one principal element, contain five or more principal elements each with the concentration between 5 and 35 atomic percentages (at. pct).[1] The basic principle of HEAs is that high mixing entropies of solid phases enhance the phase stability.[2] It is noted that Yeh,[1] Cantor,[3] and Ranganathan[4] published their own research, which opened the area of HEAs.

In 1981, Cantor *et al.*[3] conducted the first research in this brand-new field, and summarized the results in their paper. Here, they mixed several components with equal proportions and found that the composition of $Fe_{20}Cr_{20}Ni_{20}Mn_{20}Co_{20}$ formed a single face-centered-cubic (FCC) phase. They also reported that a wide range of equiatomic multi-component alloys with six to nine elements exhibit an FCC dendritic phase, which can dissolve a great deal of other transition elements, such as Nb, Ti, and V. Furthermore, Cantor *et al.* claimed that the total number of phases is below the maximum number of equilibrium phases allowed by the Gibbs-phase rule. Moreover, the same quantity is even further below the maximum number allowed under non-equilibrium solidification conditions.[3]

Since 1995, Yeh *et al.*[1] have studied the multi-principal element alloys independently in which they made groundbreaking achievements on the exploration of HEAs. They mentioned that the high mixing entropy could play an important role in reducing the number of phases in the high-order alloys, thereby improving the properties of the material.[2] It is Yeh who first introduced the "HEA concept" by providing experimental results and related theory on the subject.[1] In doing so, he opened a brand-new discipline in the field of materials science. As he mentioned, an arbitrary choice of a group of 13 miscible elements enables the design of 7099 HEA systems with 5 to 13 components. Therefore, based on his groundbreaking work, Yeh is generally recognized as the father of HEAs.

B. *Definition of HEAs*

Yeh[5] has provided two definitions for HEAs, the first of which is based on the composition of alloys, *i.e.*, HEAs are alloys containing at least five principal elements with an atomic percentage between 5 and 35 pct for each element. Additionally, the atomic percentage of each minor element, if any, is less than 5 pct. The second definition is based on the concept of configurational entropy, *i.e.*, HEAs are alloys having

ZONGYANG LYU, CHANHO LEE, SHAO-YU WANG, XUESONG FAN, and PETER K. LIAW are with the Department of Materials Science and Engineering, The University of Tennessee, Knoxville, TN 37996. Contact e-mail: pliaw@utk.edu JIEN-WEI YEH is with the Department of Materials Science and Engineering, National Tsing Hua University, Hsinchu 30013, Taiwan.

Manuscript submitted October 27, 2017.
Article published online October 25, 2018

configurational entropies in the random state, larger than 1.5 R, where R is the ideal gas constant, no matter a single-phase or multi-phase alloy forms at room temperature. As a comparison, medium entropy alloys (MEAs) are those having configurational entropies in the random state between 1 and 1.5 R and mainly corresponds to materials, which have three to four principal components.

It is worth mentioning that there are several ways to describe HEAs and MEAs, such as multi-principal element alloys (MPEAs), complex concentrated alloys (CCAs), compositionally complex alloys (CCAs), baseless alloys (BAs), and metal buffets (MBs), which are concerned about the size of the compositional space instead of the scale of entropy or the types of phases.[6–10]

C. *Mechanical Behavior of HEAs*

In general, the mechanical behavior of a material includes the hardness, yield strength, ultimate strength, plasticity, fatigue, fracture toughness, creep, which are important for structural applications. Since their inception, HEAs have shown excellent mechanical properties.[1,11–30] For example, the $CuCoNiCrAl_xFe$ HEA system studied by Yeh *et al.* can achieve a hardness of 655 HV.[1] Gludovatz *et al.*[19] compared HEAs with other major material classes in terms of fracture toughness and yield strength. It was found that the CrMnFeCoNi HEA exhibited better toughness than most pure metals and metallic alloys and possesses a strength comparable to that of structural ceramics and close to that of some bulk metallic glasses.[19]

Furthermore, HEAs, such as the $Al_{0.5}CoCrCuFeNi$ HEA, as reported by Hemphill *et al.*[17] and Tang *et al.*,[31] show promising fatigue resistance. Hemphill *et al.* put forward a fatigue ratio (fatigue-endurance limit/ultimate tensile strength) to compare the fatigue properties of HEAs with other materials with respect to the ultimate tensile strengths (UTS). It is also believed that the fatigue ratios of HEAs could exceed those of conventional alloys, such as steels, aluminum, nickel, and titanium alloys as well as bulk metallic glasses.[17]

Even though there are several review papers[5–7,32–44] for HEAs, which include discussions on their mechanical properties, it is still necessary to have a review on the mechanical behavior due to the rapid development and wide attention in this emerging area of this material system. Thus, to have a clear overview of the mechanical behavior of HEAs, we will review the previous studies on this topic.

This article is divided into two parts which feature different viewpoints, *i.e.*, the constituent-element and fabrication-method effects on the mechanical behavior of HEAs. We summarized a wide range of HEA systems in terms of their different compositions, mechanical properties, and preparation conditions using figures and tables. As a result of this endeavor, we provide a coefficient which quantifies the average influence of each element on the mechanical properties of HEAs. It is expected that the above work will enable people to have a clearer understanding regarding the mechanical properties of HEAs. The results of this study will also aid researchers, to a certain extent, in picking more useful compositions. Finally, the fabrication-method results may help future researchers prepare materials, which could meet different demands.

II. ELEMENTAL EFFECTS ON MECHANICAL BEHAVIOR OF HEAS

A. *Post-transition Metals (Al)*

Al is thought to be one of the most common components or minor elements in HEAs. It is also believed that the addition of Al can influence the mechanical behaviors of HEAs, such as hardness, compressive yield strength, tensile yield strength, and plastic strain.

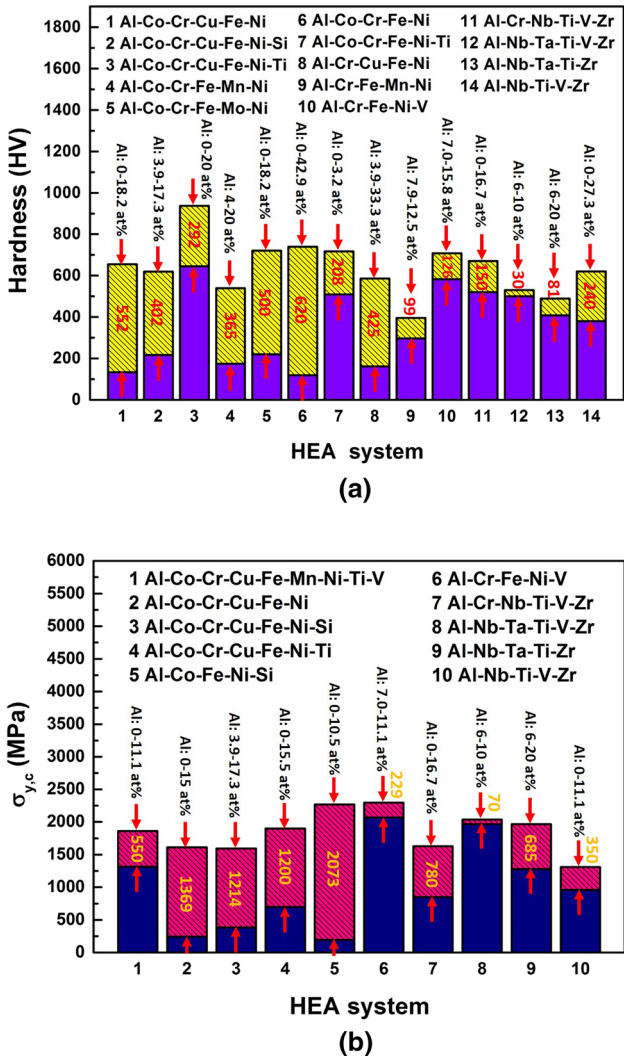

Fig. 1—Values of (*a*) hardnesses of 14 HEA systems[12,13,45–63] and (*b*) compressive yield strengths of 10 HEA systems[45,47,54,59–61,64–68] with the corresponding Al-content ranges. The hatched regions are the hardness-change ranges and compressive yield-strength-change ranges of different HEA systems, in (a) and (b), respectively. The colored numbers are the corresponding values of the change ranges (Color figure online).

Table I. Mechanical Properties of HEAs with Different Al Contents in Various Alloy Systems Refs. [12], [13], [45] through [67]

System	Composition	Hardness (HV)	$\sigma_{y,c}$ (MPa)	$\sigma_{max,c}$ (MPa)	$\varepsilon_{p,c}$ (Pct)	$\sigma_{y,t}$ (MPa)	$\sigma_{max,t}$ (MPa)	$\varepsilon_{p,t}$ (Pct)	Material Preparation Condition	Reference
Al-Co-Cr-Cu-Fe-Mn-Ni-Ti-V	$Al_0CoCrCuFeMnNiTiV$	—	1312	1312	0	—	—	—	AIIC	65
	$Al_{11.1}(CoCrCuFeMnNiTiV)_{88.9}$	—	1862	2431	0.95	—	—	—		
	$Al_{20}(CoCrCuFeMnNiTiV)_{80}$	—	1465	2016	2.35	—	—	—		
	$Al_{40}(CoCrCuFeMnNiTiV)_{60}$	—	1461	1461	0	—	—	—		
Al-Co-Cr-Cu-Fe-Ni	$Al_{0.5}CoCrCuFeNi$	208,223	487	∞	∞	—	—	—	AC	12, 52
	$Al_{1.0}CoCrCuFeNi$	356	—	—	—	—	—	—		
	$Al_{2.0}CoCrCuFeNi$	560	—	—	—	—	—	—		
	$Al_8Co_{17}Cr_{17}Cu_8Fe_{17}Ni_{33}$	—	—	—	—	357	459	9	IC	53
	$Al_0CoCrCuFeNi$	133	244	∞	∞	—	—	—	AC	54, 66
	$Al_{0.25}CoCrCu_{0.75}FeNi$	—	309	∞	∞	—	—	—		
	$Al_{0.5}CoCrCu_{0.5}FeNi$	298.5	433	∞	∞	—	—	—		
	$Al_{0.75}CoCrCu_{0.25}FeNi$	—	1613	2247	11.38	—	—	—		
	$Al_{1.0}CoCrCu_0FeNi$	—	1497	2823	26.6	—	—	—		
	$AlCoCrCuFeNi$	420	—	—	—	—	—	—	AC	13
	$AlCo_{0.5}CrCuFeNi$	437	—	—	—	—	—	—		
	$AlCoCr_{0.5}CuFeNi$	367	—	—	—	—	—	—		
	$AlCoCrCu_{0.5}FeNi$	458,665	—	—	—	—	—	—		
	$AlCoCrCuFe_{0.5}Ni$	418	—	—	—	—	—	—		
	$AlCoCrCuFeNi_{0.5}$	423	—	—	—	—	—	—		
	$Al_{1.5}CoCrCu_{0.5}FeNi$	618	—	—	—	—	—	—		
Al-Co-Cr-Cu-Fe-Ni-Si	$Al_{0.2}CoCrCu_{0.8}FeNiSi_{0.2}$	217	382	∞	∞	—	—	—	AC or AIIC	45
	$Al_{0.4}CoCrCu_{0.6}FeNiSi_{0.2}$	289	463	∞	∞	—	—	—		
	$Al_{0.5}CoCrCu_{0.5}FeNiSi_{0.2}$	314	543	2880	47.6	—	—	—		
	$Al_{0.6}CoCrCu_{0.4}FeNiSi_{0.2}$	378	914	2476	26.3	—	—	—		
	$Al_{0.8}CoCrCu_{0.2}FeNiSi_{0.2}$	595	1585	2823	13.8	—	—	—		
	$Al_{0.9}CoCrCu_{0.1}FeNiSi_{0.2}$	619	1596	3366	23.1	—	—	—		
Al-Co-Cr-Cu-Fe-Ni-Ti	$Al_0CoCrCuFeNiTi_{0.5}$	—	700	1650	28.7	—	—	—	AC	67
	$Al_{0.25}CoCrCu_{0.75}FeNiTi_{0.5}$	—	750	1970	38.5	—	—	—		
	$Al_{0.5}CoCrCu_{0.5}FeNiTi_{0.5}$	—	1580	2389	17.4	—	—	—		
	$Al_{0.75}CoCrCu_{0.25}FeNiTi_{0.5}$	—	1900	2697	12	—	—	—		
	$Al_0CoCrCuFeNiTi$	645	—	—	—	—	—	—	AC	48
	$Al_{0.5}CoCrCuFeNiTi$	757	—	—	—	—	—	—		
	$Al_{1.0}CoCrCuFeNiTi$	890	—	—	—	—	—	—		
	$Al_{1.5}CoCrCuFeNiTi$	937	—	—	—	—	—	—		
	$Al_{2.0}CoCrCuFeNiTi$	864	—	—	—	—	—	—		
Al-Co-Cr-Cu-Fe-Ni-Ti-V	$AlCoCrCuFeNiTiV$	560	—	—	—	—	—	—	AC	52
Al-Co-Cr-Cu-Ni	$AlCoCrCu_{0.5}Ni$	496	—	—	—	—	—	—		
Al-Co-Cr-Fe-Mn-Ni	$Al_0(CoCrFeMnNi)_{100}$	174	—	—	—	211	497	61.7	AC	49
	$Al_2(CoCrFeMnNi)_{98}$	179	—	—	—					
	$Al_4(CoCrFeMnNi)_{96}$	172	—	—	—	222	503	58.7		
	$Al_7(CoCrFeMnNi)_{93}$	182	—	—	—	242	529	47.2		
	$Al_8(CoCrFeMnNi)_{92}$	182	—	—	—	282	648	34.3		
	$Al_9(CoCrFeMnNi)_{91}$	222	—	—	—	336	735	27.7		
	$Al_{10}(CoCrFeMnNi)_{90}$	278	—	—	—	529	999	15.1		
	$Al_{11}(CoCrFeMnNi)_{89}$	398	—	—	—	835	1,172	3.0		

Table I. continued

System	Composition	Hardness (HV)	$\sigma_{y,c}$ (MPa)	$\sigma_{max,c}$ (MPa)	$\varepsilon_{p,c}$ (Pct)	$\sigma_{y,t}$ (MPa)	$\sigma_{max,t}$ (MPa)	$\varepsilon_{p,t}$ (Pct)	Material Preparation Condition	Reference
	$Al_{12}(CoCrFeMnNi)_{88}$	483	—	—	—	—	—	—		
	$Al_{13}(CoCrFeMnNi)_{87}$	526	—	—	—	—	—	—		
	$Al_{14}(CoCrFeMnNi)_{86}$	538	—	—	—	—	—	—		
	$Al_{15}(CoCrFeMnNi)_{85}$	531	—	—	—	—	—	—		
	$Al_{16}(CoCrFeMnNi)_{84}$	536	—	—	—	—	—	—		
	$Al_{20}(CoCrFeMnNi)_{80}$	539	—	—	—	—	—	—		
Al-Co-Cr-Fe-Mo-Ni	$Al_0CoCrFeMo_{0.5}Ni$	220	—	—	—	—	—	—	AC	62
	$Al_{0.5}CoCrFeMo_{0.5}Ni$	450	—	—	—	—	—	—		
	$Al_{1.0}CoCrFeMo_{0.5}Ni$	720	—	—	—	—	—	—		
	$Al_{1.5}CoCrFeMo_{0.5}Ni$	640	—	—	—	—	—	—		
	$Al_{2.0}CoCrFeMo_{0.5}Ni$	615	—	—	—	—	—	—		
Al-Co-Cr-Fe-Ni	$Al_0CoCrFeNi$	119	—	—	—	—	—	—	AC	46, 55, 56, 63
	$Al_{0.1}CoCrFeNi$	119	—	—	—	—	—	—		
	$Al_{0.2}CoCrFeNi$	126	—	—	—	—	—	—		
	$Al_{0.3}CoCrFeNi$	130,147	—	—	—	170	340	58.4		
	$Al_{0.4}CoCrFeNi$	196	—	—	—	—	—	—		
	$Al_{0.5}CoCrFeNi$	240	—	—	—	—	—	—		
	$Al_{0.7}CoCrFeNi$	337	—	—	—	—	—	—		
	$Al_{0.8}CoCrFeNi$	389	—	—	—	—	—	—		
	$Al_{0.9}CoCrFeNi$	528	—	—	—	—	—	—		
	$Al_{1.0}CoCrFeNi$	501,505	—	—	—	—	—	—		
	$Al_{1.2}CoCrFeNi$	479	—	—	—	—	—	—		
	$Al_{1.5}CoCrFeNi$	481,574	—	—	—	—	—	—		
	$Al_{1.8}CoCrFeNi$	486	—	—	—	—	—	—		
	$Al_{2.0}CoCrFeNi$	505,610	—	—	—	—	—	—		
	$Al_{2.5}CoCrFeNi$	695	—	—	—	—	—	—		
	$Al_{3.0}CoCrFeNi$	739	—	—	—	—	—	—		
Al-Co-Cr-Fe-Ni-Ti	$Al_0Co_{1.5}CrFeNi_{1.5}Ti_{0.5}$	509	—	—	—	—	—	—	ACH	51
	$Al_{0.2}Co_{1.5}CrFeNi_{1.5}Ti_{0.5}$	487	—	—	—	—	—	—		
	$Al_0Co_{1.5}CrFeNi_{1.5}Ti$	654	—	—	—	—	—	—		
	$Al_{0.2}Co_{1.5}CrFeNi_{1.5}Ti$	717	—	—	—	—	—	—		
	$Al_0CoCrFeNiTi$	—	—	2020	9.0	—	—	—	AC	68
	$Al_{0.5}CoCrFeNiTi$	—	—	1600	9.9	—	—	—		
	$Al_{1.0}CoCrFeNiTi$	—	—	2280	6.4	—	—	—		
	$Al_{1.5}CoCrFeNiTi$	—	—	2110	9.8	—	—	—		
	$Al_{2.0}CoCrFeNiTi$	—	—	1030	5.2	—	—	—		
Al-Co-Fe-Ni-Si	$Al_0CoFeNiSi_0$	—	194	∞	∞	—	—	—	AC	64
	$Al_{0.1}CoFeNiSi_{0.1}$	—	251	∞	∞	—	—	—		
	$Al_{0.2}CoFeNiSi_{0.2}$	—	342	∞	∞	—	—	—		
	$Al_{0.3}CoFeNiSi_{0.3}$	—	1,133	2,854	29.1	—	—	—		
	$Al_{0.4}CoFeNiSi_{0.4}$	—	2,267	2,267	0	—	—	—		
	$Al_{0.5}CoFeNiSi_{0.5}$	—	2,038	2,038	0	—	—	—		
	$Al_{0.8}CoFeNiSi_{0.8}$	—	1,001	1,001	0	—	—	—		

Table I. continued

System	Composition	Hardness (HV)	$\sigma_{y,c}$ (MPa)	$\sigma_{max,c}$ (MPa)	$\varepsilon_{p,c}$ (Pct)	$\sigma_{y,t}$ (MPa)	$\sigma_{max,t}$ (MPa)	$\varepsilon_{p,t}$ (Pct)	Material Preparation Condition	Reference
Al-Cr-Cu-Fe-Ni	$Al_{0.2}CrCuFeNi_2$	161	—	—	—	—	—	—	AC or ACR	50, 57
	$Al_{0.3}CrCuFeNi_2$	170	—	—	—	—	—	—		
	$Al_{0.4}CrCuFeNi_2$	198	—	—	—	—	—	—		
	$Al_{0.5}CrCuFeNi_2$	193,238	—	—	—	1055	1179	2		
	$Al_{0.6}CrCuFeNi_2$	278	—	—	—	—	—	—		
	$Al_{0.7}CrCuFeNi_2$	291	—	—	—	—	—	—		
	$Al_{0.8}CrCuFeNi_2$	315	—	—	—	—	—	—		
	$Al_{0.9}CrCuFeNi_2$	339	—	—	—	—	—	—		
	$Al_{1.0}CrCuFeNi_2$	315,393	—	—	—	—	—	—		
	$Al_{1.2}CrCuFeNi_2$	520	—	—	—	—	—	—		
	$Al_{1.4}CrCuFeNi_2$	547	—	—	—	—	—	—		
	$Al_{1.6}CrCuFeNi_2$	552	—	—	—	—	—	—		
	$Al_{1.8}CrCuFeNi_2$	549	—	—	—	—	—	—		
	$Al_{2.0}CrCuFeNi_2$	476,568	—	—	—	—	—	—		
	$Al_{2.2}CrCuFeNi_2$	578	—	—	—	—	—	—		
	$Al_{2.5}CrCuFeNi_2$	596	—	—	—	—	—	—		
Al-Cr-Fe-Mn-Ni	$Al_{0.3}CrFeMnNi_{0.5}$	297	—	—	—	—	—	—	AC	58
	$Al_{0.5}CrFeMnNi_{0.5}$	396	—	—	—	—	—	—		
Al-Cr-Fe-Ni-V	$Al_{0.3}CrFeNiV$	708	2067	3073	9.2	—	—	—	AC	59
	$Al_{0.5}CrFeNiV$	680	2296	2766	8.9	—	—	—		
	$Al_{0.75}CrFeNiV$	582	—	—	—	—	—	—		
	$Al_{1.0}CrFeNiV$	640	—	—	—	—	—	—		
	$Al_{1.5}CrFeNiV$	694	—	—	—	—	—	—		
Al-Cr-Nb-Ti-V-Zr	$Al_0CrNbTiVZr$	520	1260	1270	0.2	—	—	—	AC	60
	$Al_{0.25}CrNbTiVZr$	650	1095	1095	0	—	—	—		
	$Al_{0.5}CrNbTiVZr$	660	1630	1630	0	—	—	—		
	$Al_{1.0}CrNbTiVZr$	670	850	850	0	—	—	—		
Al-Nb-Ta-Ti-V-Zr	$Al_{0.3}NbTa_{0.8}Ti_{1.4}V_{0.2}Zr_{1.3}$	500	1965	2061	5.0	—	—	—	AC or ACHIP	47
	$Al_{0.5}NbTa_{0.8}Ti_{1.5}V_{0.2}Zr$	530	2035	2105	4.5	—	—	—		
Al-Nb-Ta-Ti-Zr	$AlNb_{1.5}Ta_{0.5}Ti_{1.5}Zr_{0.5}$	408	1280	1367	3.5	—	—	—		
	$Al_{0.3}NbTaTi_{1.4}Zr_{1.3}$	489	1965	2054	5.0	—	—	—		
Al-Nb-Ti-V-Zr	$Al_0NbTiVZr$	380	1320	1470	4.2	—	—	—	ACH	61
	$Al_{0.5}NbTiVZr$	470	960	1100	4	—	—	—		
	$Al_{1.0}NbTiVZr$	540	1080	1210	2.3	—	—	—		
	$Al_{1.5}NbTiVZr$	620	1310	1310	0	—	—	—		

To provide a better understanding of how much Al affects the hardness in different HEA systems, we summarized the hardness of these HEA systems in Figure 1(a).[12,13,45–63] As can be seen, Al can make a huge difference in hardness for most HEA systems, such as Al-Co-Cr-Cu-Fe-Ni,[12] Al-Co-Cr-Cu-Fe-Ni-Si,[45] Al-Co-Cr-Fe-Mo-Ni,[62] Al-Co-Cr-Fe-Ni.[46] Especially for the Al-Co-Cr-Cu-Fe-Ni[12] and Al-Co-Cr-Fe-Ni[46] systems, the hardness change could have a range of 552 and 620 HV influenced by the amount of Al added, respectively. There are also some systems with relatively small effects caused by the Al addition, such as Al-Nb-Ta-Ti-V-Zr[47] and Al-Nb-Ta-Ti-Zr,[47] whose hardness-change ranges are 30 and 81 HV, respectively.

For compressive properties, the plot of the summarized compressive yield strength, $\sigma_{y,c}$, of 10 HEA systems, in Figure 1(b),[45,47,54,59–61,64–68] shows the effect of the Al addition on the different systems, respectively. For instance, the influence of the Al addition on $\sigma_{y,c}$ could be very large, such as the Al-Co-Fe-Ni-Si[64] system whose variable range of $\sigma_{y,c}$ is 2,073 MPa. On the other hand, the effect of the Al addition on $\sigma_{y,c}$ in some systems tends to be small. For example, the Al-Nb-Ta-Ti-V-Zr[47] system whose variation range of $\sigma_{y,c}$ is about 70 MPa. The addition of Al will decrease the yield strength, as well as the hardness, in the Al-Cr-Fe-Ni-V HEA system. In Table I,[12,13,45–67] more numerical data of the mechanical properties and the preparation conditions of the HEAs in this section are summarized.

The mechanism for how Al affects the mechanical behavior can be summarized in three aspects. One aspect pertains to how the addition of Al can influence phase transformation. The capabilities of Al, as the BCC stabilizer, to combine with another element, have the order of Ni > Co > Mn > Fe > Cr,[69] *e.g.*, Ni has the largest interaction with Al. For instance, in the Al-Co-Cr-Cu-Fe-Ni[13] system, as Al is added, the phase transformed from the ductile FCC to strong BCC phases accompanied with the emergence of excellent comprehensive mechanical properties. The microstructures of HEAs with different compositions within the Al-Co-Cr-Cu-Fe-Ni system are shown in Figure 2.[13] In Figures 2(c) through (d), the $Al_{0.5}CoCrCuFeNi$ with a low Al content is composed of an FCC phase, while

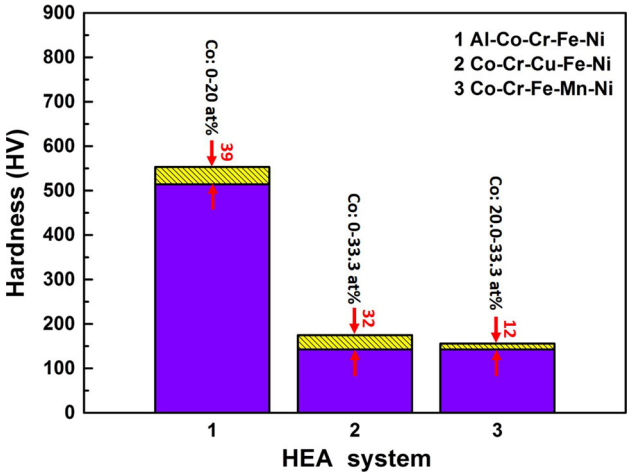

Fig. 3—Values of hardnesses of 3 HEA systems with the corresponding Co-content ranges.[70,71] The hatched regions are the hardness ranges of different HEA systems, and the colored numbers are the corresponding values of the change ranges.

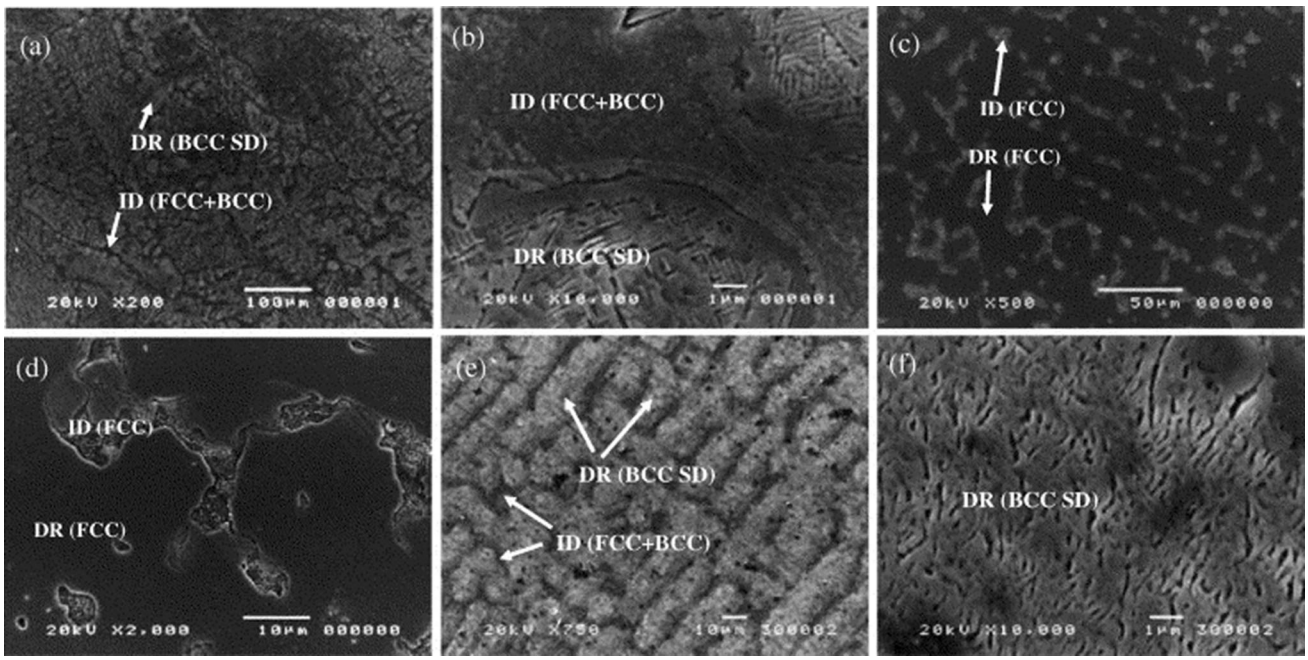

Fig. 2—The microstructures of (*a*) and (*b*) AlCoCrCuFeNi, (*c*) and (*d*) Al0.5CoCrCuFeNi, (*e*) and (*f*) AlCo0.5CrCuFeNi, where DR: dendrite, ID: interdendrite, SD: spinodal decomposition, from Ref. [13] with permission.

Figures 2(a) through (b) through (e) through (f) show that the HEAs with a higher amount of Al have a BCC phase in the dendrite and an FCC + BCC phase in the interdendrite. The reason behind the enhanced strength of the BCC phase, as compared to the FCC phase, can be explained by the basic structure factor and the solution-hardening mechanism. The similar strengthening effect of the Al addition caused by influencing the phase transformation is also reported in Al-Co-Cr-Cu-Fe-Mn-Ni-Ti-V,[65] Al-Co-Cr-Cu-Fe-Ni-Si,[45] Al-Co-Cr-Cu-Fe-Ni-Ti,[48] Al-Co-Cr-Fe-Mn-Ni,[49] and Al-Cr-Cu-Fe-Ni,[50] *etc*., HEA systems.

Another aspect is the solid-solution strengthening of Al. For the solution hardening, Tung *et al*. claimed that the dissolution of Al, which is the strongest binding element within the BCC lattice, increases the Young's modulus and slip resistance, and the large atom, Al, could greatly enlarge the lattice distortion and slip resistance.[13]

Moreover, some researchers also proposed their own explanation of Al effects. For example, Zhang *et al*.[64] hypothesized that the increase of the strength with the addition of Al is related to the atomic-packing efficiency and the lattice-distortion energy. Yeh *et al*.[5] also suggested that in the Al-Co-Cr-Fe-Ni system, the Al addition could make a contribution to achieving a finest decomposed and interconnected structure, which will lead to a high hardness of 527 HV. Tang *et al*.[69] explained the effect of Al addition at the atomic level. They explained that the electronic structures could be altered by adding Al, which will then influence the lattice structures and properties. This is thought to occur since Al has the electron configuration of $3s^2 3p^1$ with three electrons in the outer most shell, leading to a small work function, and high ionization tendency. In this case, Al, which has a high electron density and Fermi level, tends to form covalent bonds by transferring electrons to the transition metals, such as Ni, Co, Fe, and Cr. Therefore, the strong covalent bonds and the hard-atomic clusters created by Al and its surrounding transition metal atoms could lead to solution hardening.

However, the addition of Al does not always have the strengthening effect. In some HEA systems, an excessive amount of Al will have deleterious effects on its mechanical properties. For example, in the Al-Co-Cr-Fe-Mo-Ni system, Hsu *et al*.[62] found that with the additions of 0.5 at. pct (Al-0.5) and 1.0 at. pct (Al-1.0) Al, led to the formation, respectively, of hard σ-(Fe,Co, Ni)(Cr,Mo) and B2 phases, and a corresponding increase in the hardness. However, the hardness declined with the addition of 1.5 at. pct Al (Al-1.5) and further decreased with Al-2.0. Hsu *et al*.[62] concluded that the reasons for the hardness drop were (1) the reduction of the amount of the σ phase accompanied with the increase of the B2 phase in Al-1.0 and (2) the replacement of the hard σ phase with the softer BCC phase in Al-2.0. Sometimes, adding Al can result in a drop of hardness directly, even with a small amount. For instance, in the Al-Co-Cr-Fe-Ni-Ti system studied by Chuang *et al*.,[51] where the added Ti content is 0.5 at. pct, the hardness value declined, as the Al addition increased from 0 to 0.2 at. pct.

Finally, there is another important point that needs to be mentioned, *i.e*., in most of HEA systems, the addition of Al will lead to an increase in the hardness and strength accompanied with a reduction of plasticity. For example, in the Al-Co-Cr-Fe-Mn-Ni system studied by He *et al*.,[49] the authors found that the ultimate tensile strain decreased gradually from 58.7 to 3.0 pct, as the content of Al raised from 4 to 11 at. pct. Nevertheless, there also are some exceptions. For instance, in the Al-Co-Cr-Cu-Fe-Mn-Ni-Ti-V system, as studied by Zhou *et al*.,[65] the ultimate tensile strain increased from 0 to 2.35 pct with increasing Al.

Table II. Mechanical Properties of HEAs with Different Co Contents in Various Alloy Systems Refs. [70], [71]

System	Composition	Hardness (HV)	Preparation Condition	Reference
Al-Co-Cr-Fe-Ni	$(AlCrFeNi)_{100}Co_0$	553	AC	71
	$(AlCrFeNi)_{95}Co_5$	551		
	$(AlCrFeNi)_{90}Co_{10}$	535		
	$(AlCrFeNi)_{80}Co_{20}$	514		
	$(AlCrFeNi)_{66.7}Co_{33.3}$	532		
Co-Cr-Cu-Fe-Ni	$(CrCuFeNi)_{100}Co_0$	143	AC or IC	70, 71
	$(CrCuFeNi)_{95}Co_5$	146		
	$(CrCuFeNi)_{90}Co_{10}$	150		
	$(CrCuFeNi)_{85}Co_{15}$	158		
	$(CrCuFeNi)_{66.7}Co_{33.3}$	175		
	$Co_{0.5}CrCuFeNi$	158		
	$Co_{1.0}CrCuFeNi$	160		
	$Co_{1.5}CrCuFeNi$	157		
	$Co_{2.0}CrCuFeNi$	156		
Co-Cr-Fe-Mn-Ni	$(CrFeMnNi)_{100}Co_0$	148	AC	71
	$(CrFeMnNi)_{95}Co_5$	149		
	$(CrFeMnNi)_{90}Co_{10}$	146		
	$(CrFeMnNi)_{85}Co_{15}$	154		
	$(CrFeMnNi)_{80}Co_{20}$	143		
	$(CrFeMnNi)_{66.7}Co_{33.3}$	156		

In summary, the addition of Al can affect the mechanical behavior of HEAs in three ways, *i.e.*, influencing phase transformation, introducing solid-solution strengthening, and modifying the phase structure. In most HEA systems, adding Al within an appropriate amount will lead to some increase of mechanical properties. However, it can also result in the reduction of certain mechanical properties in some HEA systems.

B. *Transition Metals*

1. *Co effects on mechanical behavior of HEAs*

As shown in Figure 3,[70,71] the Co content has small effects on the hardness of Al-Co-Cr-Fe-Ni, Co-Cr-Cu-Fe-Ni, and Co-Cr-Fe-Mn-Ni HEA systems.[70,71] The variations of the hardness for both BCC and FCC HEAs are very small without an obvious trend. With increasing the addition of Co, there could be a small negative effect on the hardness in the Co-Cr-Cu-Fe-Ni HEA system.[70] The numerical data of mechanical properties and the preparation conditions of the HEAs in this section are summarized in Table II.[70,71]

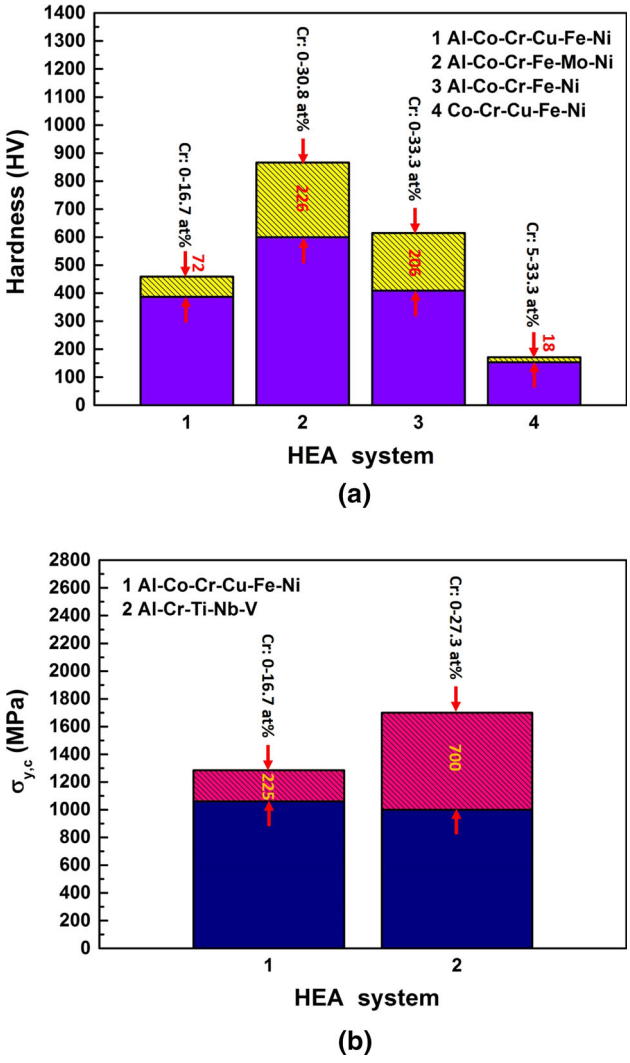

Fig. 4—Values of (*a*) hardnesses of 4 HEA systems[16,71,72] and (*b*) compressive yield strengths of 2 HEA systems[73,74] with the corresponding Cr-content ranges. The hatched regions are the hardness-change ranges and compressive yield-strength-change ranges of different HEA systems, in (a) and (b), respectively. The colored numbers are the corresponding values of the change ranges (Color figure online).

2. *Cr effects on mechanical behavior of HEAs*

The hardness, yield strength, and compressive strength of HEAs can be increased by adding Cr. The hardness of HEAs, as shown in Figure 4(a),[16,71,72] such as Al-Co-Cr-Fe-Mo-Ni[16] and Al-Co-Cr-Fe-Ni[71] systems, could be improved by more than 200 HV, as the Cr content increased. The yield strength, in the Al-Cr-Ti-Nb-V HEA system, can be enhanced by 700 MPa with the addition of Cr, as shown in Figure 4(b),[72,73] respectively, but the ultimate tensile strain is decreased from 5.2 to 0 pct.[73] Table III[16,71–73] shows the numerical data of mechanical properties and the preparation conditions of the HEAs in this section.

The two factors of the enhancing effect of Cr are (1) solid-solution strengthening and (2) second (Laves)-phase strengthening. The solid-solution strengthening of Cr in the BCC-matrix phase is due to the large lattice distortion caused by the small atomic radius of Cr.[74] For the Al-Cr-Ti-Nb-V HEA system, the strengthening rule of mixture can be expressed as:[73]

$$\sigma_{\text{alloy}} = \sigma_{\text{BCC}} \times V_{\text{BCC}} + \sigma_{\text{Laves}} \times V_{\text{Laves}}. \qquad [1]$$

In Eq. [1], σ_{alloy} is the strength of the HEA alloy; σ_{BCC} is the strength of the BCC phase; σ_{Laves} is the strength of the Laves phase; V_{BCC} and V_{Laves} are the volume fractions of the BCC and Laves phases, respectively. In the Al-Co-Cr-Fe-Mo-Ni HEA system, the strengthening effect of Cr can be attributed to the high volume fraction of the hard σ phase.[16]

However, in the Al-Co-Cr-Cu-Fe-Ni HEA system,[72] the hardness, strength, and ductility are all increased by the addition of Cr. As put forth by Xiao *et al.*, the enhancement of the comprehensive mechanical performance is caused by the ability of Cr to refine the grains of the as-cast HEA alloys.[72]

3. *Fe effects on mechanical behavior of HEAs*

The hardness ranges that are affected by the addition of Fe in 4 HEA systems are shown in Figure 5.[71,75,76] From the results of the four HEA systems, it is obvious that the Fe addition will lead to a decrease in the hardness and strength, whereas the ductility can be increased. It is because the Fe will cause the reduction of hard and topologically close-packed σ phase and the enhancement of the soft FCC phase.[75] In Table IV, more numerical data of the mechanical properties and the preparation conditions of the HEAs in this section are summarized.[71,75,76]

4. *Mn effects on mechanical behavior of HEAs*

As shown in Figure 6(a),[77] the Mn has a much greater effect on the hardness in the Co-Cr-Fe-Mn-Ni-V HEA system than in the Co-Cr-Fe-Mn-Ni HEA system. As reported by Salishchev *et al.*,[77] the Mn could cause very little deviations of atomic radii and shear moduli.

Table III. Mechanical Properties of HEAs with Different Cr Contents in Various Alloy Systems Refs. [16], [71] through [73]

System	Composition	Hardness (HV)	$\sigma_{y,c}$ (MPa)	$\sigma_{max,c}$ (MPa)	$\varepsilon_{p,c}$ (Pct)	Material Preparation Condition	Reference
Al-Co-Cr-Cu-Fe-Ni	$AlCoCr_0CuFeNi$	387	1060	1452	19.1	AC	72
	$AlCoCr_{1.0}CuFeNi$	459	1285	1857	24.6		
Al-Co-Cr-Fe-Mo-Ni	$AlCoCr_0FeMo_{0.5}Ni$	600	—	—	—	AC	16
	$AlCoCr_{0.5}FeMo_{0.5}Ni$	610	—	—	—		
	$AlCoCr_{1.0}FeMo_{0.5}Ni$	726	—	—	—		
	$AlCoCr_{1.5}FeMo_{0.5}Ni$	815	—	—	—		
	$AlCoCr_{2.0}FeMo_{0.5}Ni$	866	—	—	—		
Al-Co-Cr-Fe-Ni	$(AlCoFeNi)_{100}Cr_0$	409	—	—	—	AC	71
	$(AlCoFeNi)_{95}Cr_5$	439	—	—	—		
	$(AlCoFeNi)_{90}Cr_{10}$	479	—	—	—		
	$(AlCoFeNi)_{85}Cr_{15}$	509	—	—	—		
	$(AlCoFeNi)_{80}Cr_{20}$	514	—	—	—		
	$(AlCoFeNi)_{66.7}Cr_{33.3}$	615	—	—	—		
Al-Cr-Ti-Nb-V	$AlCr_0TiNbV$	—	1000	1280	5.2	ACH, at 1473 K	73
	$AlCr_{0.5}TiNbV$	—	1300	1430	0.8		
	$AlCr_{1.0}TiNbV$	—	1550	1570	0.4		
	$AlCr_{1.5}TiNbV$	—	1700	1700	0		
Co-Cr-Cu-Fe-Ni	$(CoCuFeNi)_{100}Cr_0$	154	—	—	—	AC	71
	$(CoCuFeNi)_{95}Cr_5$	153	—	—	—		
	$(CoCuFeNi)_{90}Cr_{10}$	158	—	—	—		
	$(CoCuFeNi)_{85}Cr_{15}$	161	—	—	—		
	$(CoCuFeNi)_{66.7}Cr_{33.3}$	171	—	—	—		

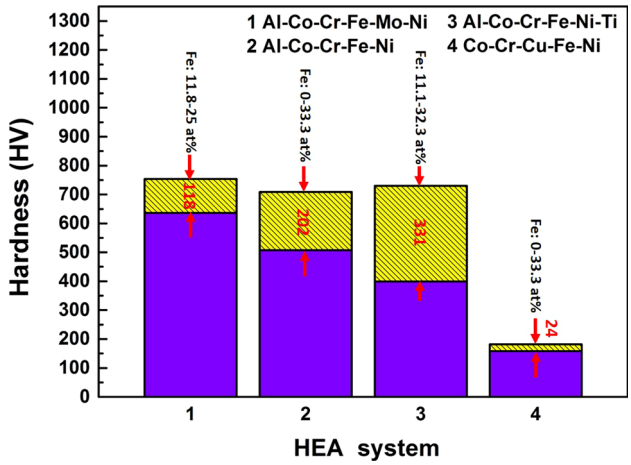

Fig. 5—Values of hardnesses of 4 HEA systems with the corresponding Fe-content ranges.[71,75,76] The hatched regions are the hardness ranges of different HEA systems, and the colored numbers are the corresponding values of the change ranges (Color figure online).

Then the low-strengthening effect in the CoCrFeNi alloy should be expected from the addition of Mn. But in the Cr-Cu-Fe-Mn-Ni HEA system, as shown in Figure 6(b),[77,78] the yield strength, tensile strength, and ultimate tensile strain are increased from 332, 608 MPa, and 19.1 pct to 441, 887 MPa, and 23.4 pct, respectively, as the Mn content is elevated from 0 to 1.0 at. pct.[78] The effects of Mn on the tensile yield strength in Cr-Cu-Fe-Mn-Ni and Co-Cr-Fe-Mn-Ni HEA systems are similar to each other. Presently, the exact reasons for the enhancement effect of Mn is not well understood and, therefore, further research is needed to gain insight into this phenomenon. The numerical data of mechanical properties and the preparation conditions of the HEAs in this section are summarized in Table V.[77,78]

5. *Mo effects on mechanical behavior of HEAs*

The element Mo can generally improve the hardness and strength in HEAs that is accompanied by a reduction in its ductility. We plot out three HEA systems in Figure 7(a),[79–82] which shows the content ranges of Mo and the corresponding hardness values in the CoCrFeMoNi, Co-Mo-Ni-V-W, and Hf-Mo-Nb-Ta-Ti-Zr HEA systems. To exhibit the effect of the Mo element on yield strength, 6 HEA systems are summarized in Figure 7(b),[80,81,83–85] from which we can observe that the effect of Mo on the Al-Co-Cr-Fe-Mo-Ni HEA system is much larger than in other HEA systems. In the Al-Co-Cr-Fe-Mo-Ni HEA system, the enhancement effect of Mo can be attributed to solid-solution strengthening, caused by the higher lattice distortion after the addition of Mo, and the precipitation of the α phase, which has a strong mutual reinforcing effect with the BCC phase due to a certain crystallographic orientation relationship between them.[83] As reported for the Co-Cr-Fe-Mo-Ni system, Mo can catalyze the precipitation of brittle but quite hard (Cr,Mo)-rich σ and (Mo,Cr)-rich μ phases in a FCC matrix,[79,80] which will increase the strength and hardness but reduce the ductility. As shown in Figures 8(a) through (b), the as-cast Mo_x (x = 0 and 0.1) have a single-phase

Table IV. Mechanical Properties of HEAs with Different Fe Contents in Various Alloy Systems Refs. [71], [75], [76]

System	Composition	Hardness (HV)	$\sigma_{y,c}$ (MPa)	$\sigma_{max,c}$ (MPa)	$\varepsilon_{p,c}$ (Pct)	Material Preparation Condition	Reference
Al-Co-Cr-Fe-Mo-Ni	$AlCoCrFe_{0.6}Mo_{0.5}Ni$	754	—	—	—	AC	76
	$AlCoCrFe_{1.0}Mo_{0.5}Ni$	731	—	—	—		
	$AlCoCrFe_{1.5}Mo_{0.5}Ni$	636	—	—	—		
	$AlCoCrFe_{2.0}Mo_{0.5}Ni$	637	—	—	—		
Al-Co-Cr-Fe-Ni	$(AlCoCrNi)_{100}Fe_0$	709	—	—	—	AC	71
	$(AlCoCrNi)_{95}Fe_5$	662	—	—	—		
	$(AlCoCrNi)_{90}Fe_{10}$	588	—	—	—		
	$(AlCoCrNi)_{85}Fe_{15}$	553	—	—	—		
	$(AlCoCrNi)_{80}Fe_{20}$	515	—	—	—		
	$(AlCoCrNi)_{66.7}Fe_{33.3}$	507	—	—	—		
Al-Co-Cr-Fe-Ni-Ti	$Al_{0.5}CoCrFe_{0.5}NiTi_{0.5}$	730	1659	2240	11	AC	75
	$Al_{0.5}CoCrFe_{1.0}NiTi_{0.5}$	526	1178	1801	21		
	$Al_{0.5}CoCrFe_{1.5}NiTi_{0.6}$	431	895	1834	38		
	$Al_{0.5}CoCrFe_{2.0}NiTi_{0.7}$	399	866	1736	45		
Co-Cr-Cu-Fe-Ni	$(CoCrCuNi)_{100}Fe_0$	182	—	—	—	AC	71
	$(CoCrCuNi)_{95}Fe_5$	181	—	—	—		
	$(CoCrCuNi)_{90}Fe_{10}$	172	—	—	—		
	$(CoCrCuNi)_{85}Fe_{15}$	171	—	—	—		
	$(CoCrCuNi)_{80}Fe_{20}$	157	—	—	—		
	$(CoCrCuNi)_{66.7}Fe_{33.3}$	158	—	—	—		

structure, while the as-cast Mo_x (x = 0.2 and 0.3) shows the emergence of a dendritic structure, as seen in Figures 8(c) through (d). In Figures 8(e) through (l), the (Cr,Mo)-rich σ and (Mo,Cr)-rich μ phases can be observed, which are further identified by TEM, shown in Figures 8(m) through (n).[79] Moreover, in the Co-Mo-Ni-V-W HEA system, Jiang *et al.*[81] found that increasing the additions of Mo and W could improve the hardness by raising the volume fractions of the hard BCC phase and eutectic microstructure. As shown in Table VI,[79–85] we summarized the numerical data of the mechanical properties and the preparation conditions of the HEAs in this section.

6. *Nb effects on mechanical behavior of HEAs*

As shown in Figure 9[86,87] which contains 2 HEA systems, in the Co-Cr-Fe-Nb-Ni HEA system,[86] the yield strength and compressive strength can be greatly improved from 423 and 2016 MPa to 1414 and 2276 MPa, respectively, by adding Nb, but with an apparent decrease in the plasticity. The reason behind the effects of Nb is attributed to the increase in the volumes of hard and brittle $Co(Ni,Fe,Cr)_2Nb$-type Laves phase arising from the increase of the content of Nb.[86,87] As shown in Figure 10, the FCC phase (marked as A) is dominant in $CoFeNi_2V_{0.5}Nb_x$ (x = 0–0.7), while the $Co(Ni,Fe,Cr)_2Nb$-type Laves phase becomes the primary phase when x reaches 0.8 and 1.0.[87] The numerical data of mechanical properties and the preparation conditions of the HEAs in this section are provided in Table VII.[86,87]

7. *Ni effects on mechanical behavior of HEAs*

As shown in Figure 11,[71,88,89] which displays results for six HEA systems, the addition of Ni reduces the hardness and strength of HEAs while increasing their ductility. These changes are thought to be induced by the ability of Ni to increase the production of the soft FCC phase.[71,88,89] For the Co-Cr-Fe-Ni HEA system, the volume fractions of the hard BCC and Cr-rich σ phases will be reduced with increasing the Ni content.[71] In the Al-Co-Cr-Fe-Mo-Ni HEA system, adding Ni will not only increase the amount of the FCC phase but also in making the B2 phase softer.[88] In Table VIII,[71,88,89] more numerical data of mechanical properties and the preparation conditions of the HEAs in this section are provided.

8. *Ti effects on mechanical behavior of HEAs*

As shown in Figures 12(a)[63,72,90–92] and 12(b),[72,91–94] which contain 6 and 7 HEA systems, respectively, the addition of Ti can increase the hardness and strength with an accompanying reduction of plasticity in most of HEA systems, such as Al-Co-Cr-Cu-Fe-Ni-Ti,[72] Al-Co-Cu-Fe-Ni-Ti,[72] Al-Fe-Mn-Ni-Ti,[90] Co-Cr-Fe-Ni-Ti,[91] Mo-Nb-Ta-Ti-V-W,[93] and Mo-Nb-Ta-Ti-W.[93] However, for the Nb-Ta-Ti-V-W HEA system,[92] adding Ti will decrease the hardness and yield strength while increasing the ductility. More numerical data of the mechanical properties and the preparation conditions of the HEAs in this section are listed in Table IX.[63,72,90–94]

The strengthening effect of Ti, as observed in Al-Co-Cr-Fe-Ni-Ti,[94] Co-Cr-Fe-Ni-Ti,[91] Mo-Nb-Ta-Ti-V-W,[93] and Mo-Nb-Ta-Ti-W [93] HEA systems, can be attributed to the solid-solution strengthening of Ti atoms. On the other hand, the addition of Ti can introduce hard phases, such as Laves-$(Co,Fe,Ni,Cr)_2Ti$, R-$(Co,Fe,Ni)_2(Ti,Cr)$, and σ-(Cr,Ti)(Co,Fe,Ni) phases,[91] which will enhance the strength of HEAs.

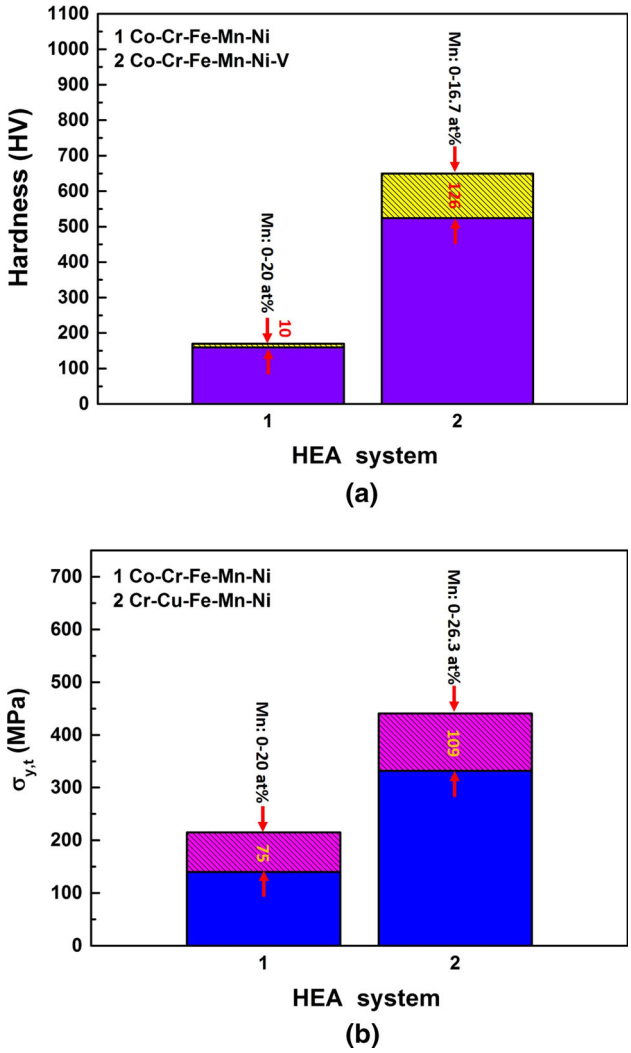

Fig. 6—Values of (*a*) hardnesses of 2 HEA systems[77] and (*b*) tensile yield strengths of 2 HEA systems[77,78] with the corresponding Mn-content ranges. The hatched regions are the hardness-change ranges and tensile yield-strength-change ranges of different HEA systems, in (a) and (b), respectively. The colored numbers are the corresponding values of the change ranges (Color figure online).

9. *V effects on mechanical behavior of HEAs*

The effects of *V* generally increase the hardness and strength, while decreasing the ductility of HEAs, as shown in Figure 13(a)[11,77,95] and Figure 13(b)[18,77,95] for 3 HEA systems. This effect is thought to be caused by phase transformations,[11] solid-solution strengthening,[77,95] and precipitation strengthening.[11] The phase transformation mainly refers to the transformation from the soft FCC to hard BCC phases, such as in the Al-Co-Cr-Cu-Fe-Ni-V HEA system.[11] The volume fraction of the precipitation phase, such as the V-rich σ phase in the Al-Co-Cr-Cu-Fe-Ni-V HEA system,[11] will increase with a corresponding increase in the V content within a certain range, which can cause a sharp enhancement of hardness. It is worth mentioning that Stepanov *et al.*[96] provide two power-law-type dependences about the effect of the (Cr,V)-rich σ phase volume fraction on the hardness and yield strength in the Co-Cr-Fe-Mn-Ni-V HEA system, respectively. For hardness, the equation[96] is

$$\mathrm{HV} = v(\sigma)^{1.45} + 142.4, \qquad [2]$$

where HV is the hardness of alloys, and v (sigma) is the volume fraction of the sigma phase. For the yield strength, the dependence is described as[96]

$$\sigma_{0.2} = v(\sigma)^{1.69} + 229.3, \qquad [3]$$

where $\sigma_{0.2}$ is the yield strength of alloys, and v (sigma) is the volume fraction of the sigma phase. In Table X, more numerical data of mechanical properties and the preparation conditions of the HEAs in this section are summarized.[11,18,77,95,142]

10. *W effects on mechanical behavior of HEAs*

Jiang *et al.*[97] studied the influence of *W* in the Cr-Fe-Ni-V-W HEA system. They found that the hardness of the $CrFeNiV_{0.5}W_x$ HEA decreases as the W content increases from 0.25 to 1.0.[97] But for the $CrFeNi_2V_{0.5}W_x$ HEA, the hardness can be rise from 223 to 305 HV with increasing the W content, which is due to the increased volume fraction of the BCC solid-solution phase.[97]

11. *Zr effects on mechanical behavior of HEAs*

The influence of Zr in the Al-Co-Cr-Fe-Ni-Zr HEA system studied by Razuan *et al.*[98] shows that the hardness can be greatly enhanced from 450 HV without the Zr addition to 858 HV with an addition of Zr (about 3.85 at. pct). But the hardness in the Al-Co-Cr-Fe-Ni-Zr HEA system will be slowly decreased with increasing the Zr content, which could be due to the variation of the phase morphology.[98]

C. *Metalloids*

1. *Si effects on mechanical behavior of HEAs*

As shown in Figures 14(a)[99,100] and 14(b)[27,100,101] which contains 2 and 3 HEA systems, respectively, the addition of Si can cause increases in the hardness and strength with a decrease of ductility in HEAs. In the Al-Co-Cr-Cu-Fe-Ni-Si HEA system, Liu *et al.*[99] attributed the enhancement of Si to the basic structure change from FCC to BCC phases and the solid-solution strengthening. In the Al-Co-Cr-Fe-Ni-Si HEA system, the reasons for the strengthening effect of Si are thought to arise from the solid solution of the Si element and precipitation strengthening of the nanoscale cellular structure.[101] The enhancing effect of Si in the Hf-Mo-Nb-Si-Ti-Zr HEA system is mainly attributed to the formation of the M_5Si_3 phase and the relatively fine cellular dendritic structure caused by the addition of Si.[100] As shown in Table XI,[27,99–101] the numerical

Table V. Mechanical Properties of HEAs with Different Mn Contents in Various Alloy Systems Refs. [77], [78]

System	Composition	Hardness (HV)	$\sigma_{y,t}$ (MPa)	$\sigma_{max,t}$ (MPa)	$\varepsilon_{p,t}$ (Pct)	Material Preparation Condition	Reference
Co-Cr-Fe-Mn-Ni	$CoCrFeMn_0Ni$	160	140	488	83	AC	77
	$CoCrFeMn_{1.0}Ni$	170	215	491	71		
Co-Cr-Fe-Mn-Ni-V	$CoCrFeMn_0NiV$	524	—	311	0		
	$CoCrFeMn_{1.0}NiV$	650	—	90	0		
Cr-Cu-Fe-Mn-Ni	$Cr_{0.4}CuFe_{0.4}Mn_0Ni$	—	332	608	19.1	ACH, at 1273 K	78
	$Cr_{0.4}CuFe_{0.4}Mn_{0.2}Ni$	—	356	741	21.9		
	$Cr_{0.4}CuFe_{0.4}Mn_{0.4}Ni$	—	401	768	21.1		
	$Cr_{0.4}CuFe_{0.4}Mn_{0.6}Ni$	—	408	764	20.5		
	$Cr_{0.4}CuFe_{0.4}Mn_{0.8}Ni$	—	428	829	20.4		
	$Cr_{0.4}CuFe_{0.4}Mn_{1.0}Ni$	—	441	887	23.4		
	$Cr_{0.4}CuFe_{0.4}Mn_{1.2}Ni$	—	386	771	19.3		
	$Cr_{0.4}CuFe_{0.4}Mn_{1.4}Ni$	—	388	662	7.3		

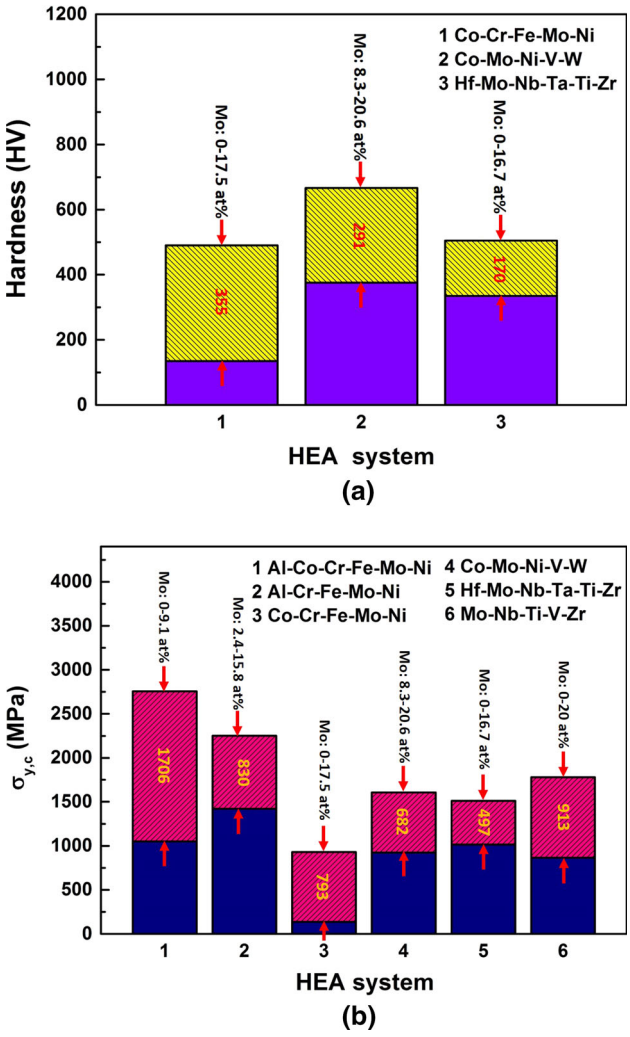

Fig. 7—Values of (*a*) hardnesses of 3 HEA systems [79–82] and (*b*) compressive yield strengths of 6 HEA systems[80,81,83–85] with the corresponding Mo-content ranges. The hatched regions are the hardness-change ranges and compressive yield-strength-change ranges of different HEA systems, in (a) and (b), respectively. The colored numbers are the corresponding values of the change ranges (Color figure online).

data of mechanical properties and the preparation conditions of the HEAs in this section are listed.

D. *Other Non-metal Elements*

1. *C effects on mechanical behavior of HEAs*

The addition of C into HEAs can generally improve the mechanical properties, as shown in Figures 15(a)[102,103] and 15(b)[104–106] containing 2 HEA systems. In the Al-C-Cr-Fe-Mn-Ni HEA system, Wang *et al*. reported that the ductility and strain hardening are increased due to the formation of the non-cell-forming structure, which is composed of the Taylor lattice, domain boundaries, and micro-bands. The yield strength is enhanced for the increased lattice friction caused by the interstitial strengthening of the solute carbon.[104] In the C-Co-Cr-Fe-Mn-Ni HEA system, Stepanov *et al*. found that the hardening effect of C can be attributed to the solid-solution strengthening of the FCC phase by carbon and carbides.[107] In the same system, Wu *et al*. attributed the increase of strain hardening and strength to the enhancement of deformation twinning.[105] More numerical data of mechanical properties and the preparation conditions of the HEAs in this section are provided in Table XII.[102–107]

III. MANUFACTURING EFFECTS ON MECHANICAL BEHAVIOR OF HEAS

A. *Bridgman Solidification*

Bridgman solidification (BS) is a better manufacturing method based on the aspect of microstructural control rather than the common casting technique. As reported in the literature, the ductility of HEAs can be improved by BS. Zhang *et al*.[108] fabricated the AlCoCrFeNi HEA by BS, and the plasticity of BS samples was increased as much as 35 pct, as compared to the samples produced by the common casting method, but the yield strength was approximately 163 MPa lower. They also found that the morphology of the AlCoCrFeNi HEA changed from dendrites to

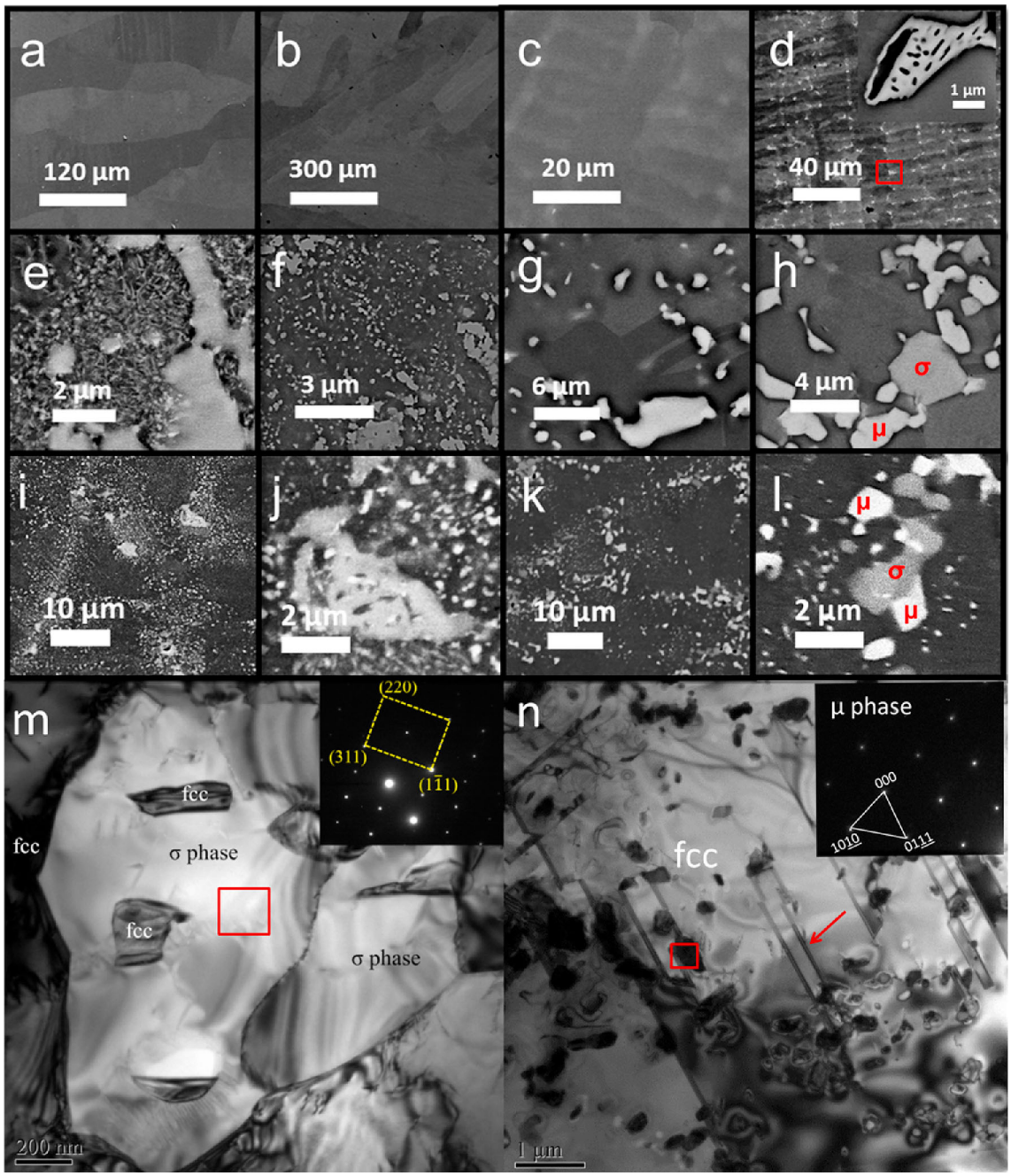

Fig. 8—SEM results of the as-cast $CoCrFeNiMo_x$: (*a*) $x = 0$, (b) $x = 0.1$, (*c*) $x = 0.2$, and (*d*) $x = 0.3$; the 60 pct-rolling $Mo_{0.3}$, annealed at (*e*) 973 K for 3 ds, (*f*) 1073 K for 3 ds, (*g*) 1173 K for 2 ds, (*h*) 1273 K for 1 days, (*i*)–(*j*) 1123 K for 1 h, (*k*)–(*l*) 1173 K for 5 h. TEM analyses of $Mo_{0.3}$ alloy, (*m*) the as-cast and (*n*) 60 pct-rolled, and annealed at 1073 K for 3 ds, from Ref. [79] with permission.

equiaxed grains, which may be caused by the longer holding time, lower heating temperature, and higher G/V (the temperature gradient-to-the growth rate ratio) value during the Bridgeman solidification.[108] The improvement of plasticity, as studied by Zhang *et al.*,[18] could be due to the release of the stress caused by the dislocation pileup, the absorption of the external energy of plastic deformation, and the hindrance to the development of cracks. The reduction of the yield strength may be ascribed to the disappearance of dendrites and more homogeneous microstructures, which will make it easier for dislocations movement.[18]

Ma *et al.*[109] fabricated a single-crystal CoCrFeNi$Al_{0.3}$, which mainly focused on the ⟨001⟩ orientation and achieved a tensile elongation of about 80 pct. The reasons behind the outstanding tensile ductility, as they

Table VI. Mechanical Properties of HEAs with Different Mo Contents in Various Alloy Systems Refs. [79] through [85]

System	Composition	Hardness (HV)	$\sigma_{y,c}$ (MPa)	$\sigma_{max,c}$ (MPa)	$\varepsilon_{p,c}$ (Pct)	$\sigma_{y,t}$ (MPa)	$\sigma_{max,t}$ (MPa)	$\varepsilon_{p,t}$ (Pct)	Material Preparation Condition	Reference
Al-Co-Cr-Fe-Mo-Ni	$AlCoCrFeMo_0Ni$	—	1051	—	—	—	—	—	AIIC	83
	$AlCoCrFeMo_{0.1}Ni$	—	1804	2280	9.1	—	—	—		
	$AlCoCrFeMo_{0.2}Ni$	—	2456	2953	3.4	—	—	—		
	$AlCoCrFeMo_{0.3}Ni$	—	2649	3208	3.3	—	—	—		
	$AlCoCrFeMo_{0.4}Ni$	—	2670	3161	3	—	—	—		
	$AlCoCrFeMo_{0.5}Ni$	—	2757	3036	2.5	—	—	—		
Al-Cr-Fe-Mo-Ni	$AlCrFeMo_{0.1}Ni$	—	1422	2035	6.2	—	—	—	MC	84
	$AlCrFeMo_{0.25}Ni$	—	1837	2058	4.2	—	—	—		
	$AlCrFeMo_{0.5}Ni$	—	2045	2397	4.6	—	—	—		
	$AlCrFeMo_{0.75}Ni$	—	2252	2612	6.7	—	—	—		
	$AlCrFeMo_{1.0}Ni$	—	—	2537	—	—	—	—		
	$AlCrFeMo_{1.25}Ni$	—	—	2582	—	—	—	—		
Co-Cr-Fe-Mo-Ni	$CoCrFeMo_0Ni$	135	136	871	75	155	472	58.9	AC	79, 80
	$CoCrFeMo_{0.1}Ni$	—	—	—	—	199	479	51.1		
	$CoCrFeMo_{0.2}Ni$	—	—	—	—	255	590	55.1		
	$CoCrFeMo_{0.3}Ni$	220	305	1269	58	305	710	49.3		
	$CoCrFeMo_{0.5}Ni$	322	510	1371	33	—	—	—		
	$CoCrFeMo_{0.85}Ni$	490	929	1441	21	—	—	—		
Co-Mo-Ni-V-W	$Co_2Mo_{0.5}Ni_2VW_{0.5}$	376	925	—	—	—	—	—	AC	81
	$Co_2Mo_{0.6}Ni_2VW_{0.6}$	560	1411	2108	11.8	—	—	—		
	$Co_2Mo_{0.8}Ni_2VW_{0.8}$	577	1431	2364	14.4	—	—	—		
	$Co_2Mo_{1.0}Ni_2VW_{1.0}$	510	1371	2209	16	—	—	—		
	$Co_2Mo_{1.5}Ni_2VW_{1.5}$	583	1320	2133	13.9	—	—	—		
	$Co_2Mo_{1.75}Ni_2VW_{1.75}$	667	1607	2313	9.4	—	—	—		
Hf-Mo-Nb-Ta-Ti-Zr	$HfMo_0NbTaTiZr$	335	1015	—	—	—	—	—	AC	82
	$HfMo_{0.25}NbTaTiZr$	395	1112	—	—	—	—	—		
	$HfMo_{0.5}NbTaTiZr$	480	1317	—	—	—	—	—		
	$HfMo_{0.75}NbTaTiZr$	492	1373	—	—	—	—	—		
	$HfMo_{1.0}NbTaTiZr$	505	1512	1,818	12	—	—	—		
Mo-Nb-Ti-V-Zr	$Mo_0NbTiVZr$	—	1104	—	50	—	—	—	AC	85
	$Mo_{0.3}NbTiVZr$	—	1289	—	42	—	—	—		
	$Mo_{0.5}NbTiVZr$	—	1473	—	32	—	—	—		
	$Mo_{0.7}NbTiVZr$	—	1760	—	32	—	—	—		
	$Mo_{1.0}NbTiVZr$	—	1779	—	32	—	—	—		
	$Mo_{1.3}NbTiVZr$	—	1496	—	30	—	—	—		
	$Mo_{1.5}NbTiVZr$	—	1603	—	20	—	—	—		
	$Mo_{1.7}NbTiVZr$	—	1645	—	15	—	—	—		
	$Mo_{2.0}NbTiVZr$	—	1765	—	12	—	—	—		
	$Mo_0NbTiV_{0.3}Zr$	—	866	—	45	—	—	—		
	$Mo_{0.1}NbTiV_{0.3}Zr$	—	932	—	45	—	—	—		
	$Mo_{0.3}NbTiV_{0.3}Zr$	—	1312	—	50	—	—	—		
	$Mo_{0.5}NbTiV_{0.3}Zr$	—	1301	—	43	—	—	—		
	$Mo_{0.7}NbTiV_{0.3}Zr$	—	1436	—	26.6	—	—	—		
	$Mo_{1.0}NbTiV_{0.3}Zr$	—	1455	—	25	—	—	—		
	$Mo_{1.3}NbTiV_{0.3}Zr$	—	1603	—	20	—	—	—		
	$Mo_{1.5}NbTiV_{0.3}Zr$	—	1576	—	8	—	—	—		

reported, are the low-angle grain boundaries, less distance to dislocation motion, single ⟨001⟩ crystal orientation, and less plastic-strain incompatibility.[109]

B. *Additive Manufacturing*

Additive manufacturing (AM), which is popularly called three-dimensional (3D) printing or rapid prototyping, is used to create something efficiently, and the output is a prototype or basic model, which can be further modified to produce the desired products. Other terms have been used to describe this technology, such as the automated fabrication (Autofab), freeform fabrication, or solid freeform fabrication, layer-based manufacturing, stereolithography, or 3D printing and rapid prototyping. If combined with other technologies to achieve the process chain, AM can greatly shorten the production time and cost.

The study of HEAs fabricated by AM has been initiated by some investigators in recent years. For instance, Brif *et al.*[110] fabricated an equiatomic FeCoCrNi HEA by selective laser melting (SLM).

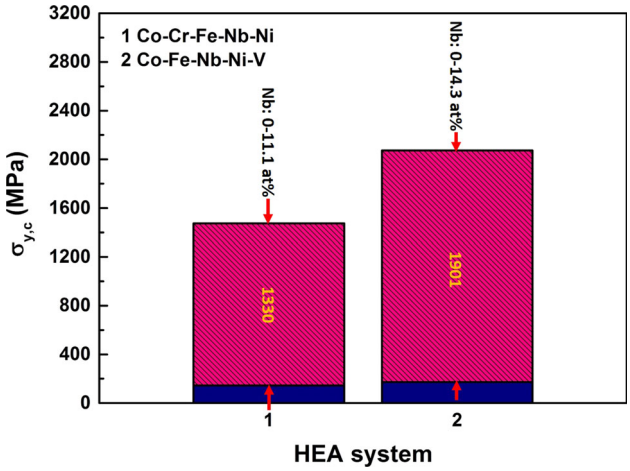

Fig. 9—Values of compressive yield strengths of 2 HEA systems with the corresponding Nb-content ranges.[86,87] The hatched regions are compressive yield strength ranges of different HEA systems, and the colored numbers are the corresponding values of the change ranges (Color figure online).

The tensile yield strength (600 MPa) is more than three times higher than that employed by the arc-melting and casting method (188 MPa) while maintaining a great portion of the ductility (with an elongation of 32 pct). Zhou *et al.*[111] prepared the carbon-containing FeCoCrNi HEA with SLM, which has the tensile yield strength of 650 MPa and elongation of 13.5 pct. The popular CoCrFeNiMn HEA was prepared using SLM by Zhu *et al.*,[112] whose tensile yield strength (~ 510 MPa) is twice that of the as-cast samples.

Using laser engineering net shaping (LENS), Kunce *et al.*[113] produced samples of the AlCoCrFeNi HEA, which exhibits an average hardness of about 543 HV0.5, which is approximately 15 pct higher than the hardness of samples in the as-cast state. The authors also announced that the laser-scan rate has significant influence on the microstructure, where it can increase the cooling rate and reduce the average grain size, and the hardness increases as the average grain size is decreased.[113]

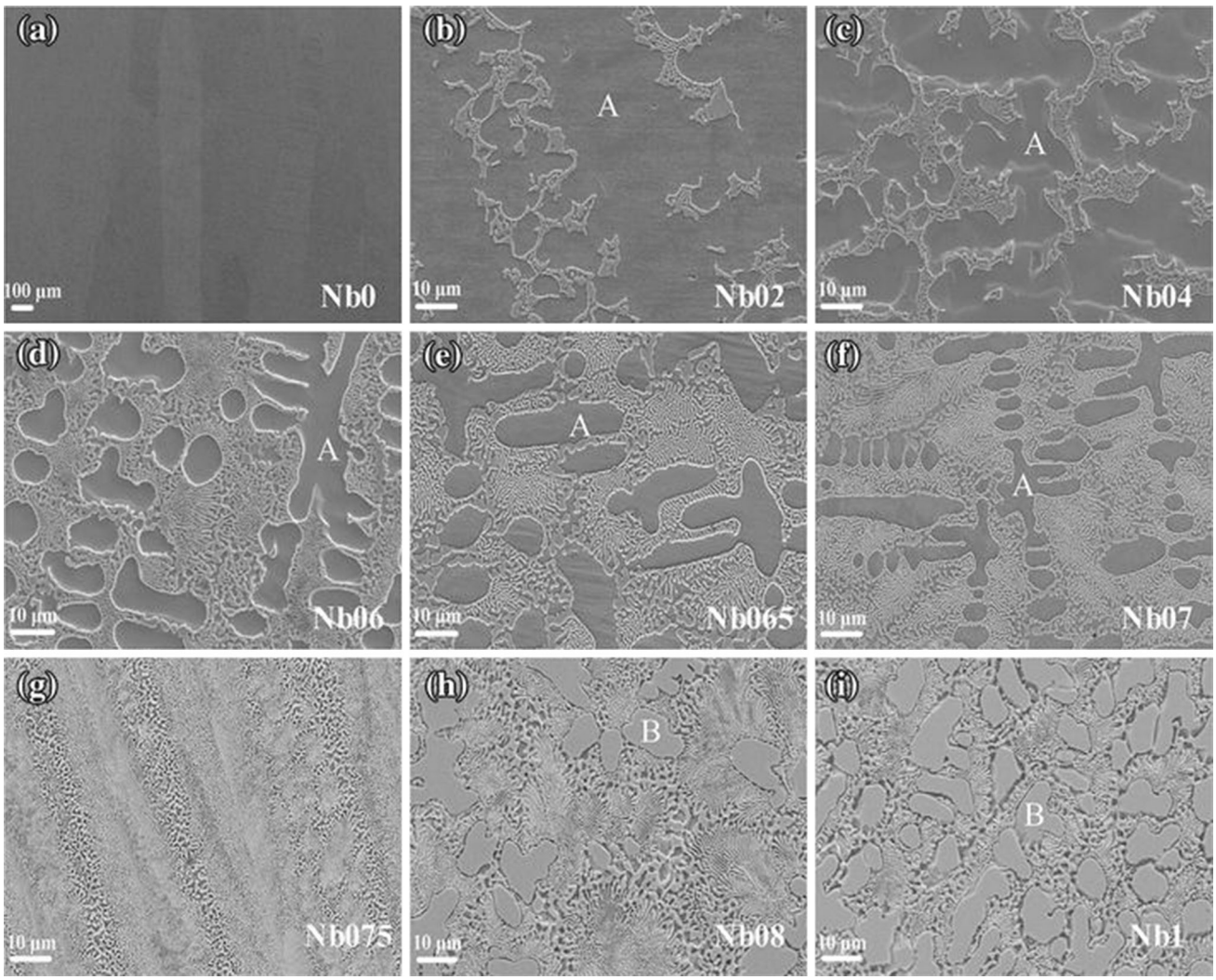

Fig. 10—The microstructure-evolution of the as-cast $CoFeNi_2V_{0.5}N_{bx}$ HEAs: (*a*) $x = 0$, (*b*) $x = 0.2$, (*c*) $x = 0.4$, (*d*) $x = 0.6$, (*e*) $x = 0.65$, (*f*) $x = 0.7$, (*g*) $x = 0.75$, (*h*) $x = 0.8$, (*i*) $x = 1.0$, from Ref. [87] with permission.

Table VII. Mechanical Properties of HEAs with Different Nb Contents in Various Alloy Systems Refs. [86], [87]

System	Composition	Hardness (HV)	$\sigma_{y,c}$ (MPa)	$\sigma_{max,c}$ (MPa)	$\varepsilon_{p,c}$ (Pct)	Material Preparation Condition	Reference
Co-Cr-Fe-Nb-Ni	$CoCrFeNb_0Ni$	—	145	—	—	AC	86
	$CoCrFeNb_{0.25}Ni$	—	423	2016	34.8		
	$CoCrFeNb_{0.45}Ni$	—	1475	2558	21.3		
	$CoCrFeNb_{0.5}Ni$	—	1414	2276	17.7		
	$CoCrFeNb_{0.75}Ni$	—	—	2078	—		
	$CoCrFeNb_{1.0}Ni$	—	—	1198	—		
	$CoCrFeNb_{1.2}Ni$	—	—	940	—		
Co-Fe-Nb-Ni-V	$CoFeNb_0Ni_2V_{0.5}$	137	172	—	—	AC	87
	$CoFeNb_{0.2}Ni_2V_{0.5}$	290	660	—	—		
	$CoFeNb_{0.4}Ni_2V_{0.5}$	361	776	2267	32.4		
	$CoFeNb_{0.6}Ni_2V_{0.5}$	499	1806	2101	7.8		
	$CoFeNb_{0.75}Ni_2V_{0.5}$	642	2073	2232	3.4		
	$CoFeNb_{1.0}Ni_2V_{0.5}$	689	2018	2280	2.5		

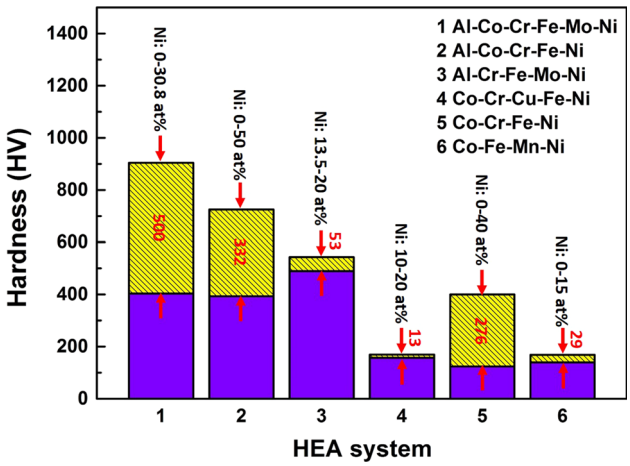

Fig. 11—Values of hardnesses of 6 HEA systems with the corresponding Ni-content ranges.[71,88,89] The hatched regions are the hardness ranges of different HEA systems, and the colored numbers are the corresponding values of the change ranges (Color figure online).

Selective electron beam melting (SEBM) was used by Fujieda *et al.*[114] to fabricate the AlCoCrFeNi HEA, where it was observed that the method markedly increased the ductility by more than three times, as compared to the as-cast condition while the compressive yield strength remained approximately the same. The greater plasticity of the SEBM samples, as compared to the as-cast condition, is mainly due to the finer microstructure introduced by the SEBM technique. The compressive yield strength of SEBM samples is also lower than that of the cast samples, which is due to the appearance of the soft FCC phase in SEBM samples. The authors also observed the anisotropy of compressive properties and found that the compressive properties of the specimens whose cylinder axes were parallel to the build direction were better than those of the specimens whose cylinder axes were perpendicular to the build direction. The reason behind the anisotropy is the large number of grain boundaries along the compression direction.[114]

Ocelík *et al.*[115] claimed that in the AlCoCrFeNi HEA system, the solidification rate of laser-beam remelting has a significant influence on the fraction, chemical composition, and spatial distribution of the FCC and BCC phases. Furthermore, the high solidification rate will increase the amount of the BCC phase that is accompanied by a relative increase in the hardness.

An equiatomic CoCrFeMnNi HEA was fabricated by Haase *et al.*[116] with laser-metal deposition (LMD), and its compressive yield strength is 260 MPa, higher than that of the HEA within the same composition that is produced using conventional casting (about 125 through 215 MPa). There are two reasons[116] for the strengthening effect of LMD as mentioned by the authors. The first reason is that the texture of the HEA by LMD may be related to a lower mean Schmid factor, which means that the initiation of dislocation movement needs a higher stress. The second one is the higher dislocation density, due to the rapid solidification and cooling, during the LMD process than that in the conventional casting process.

C. *Solid-State Manufacturing*

The method of solid-state manufacturing of HEAs mainly refers to the process of powder metallurgy, which consists of the powder fabrication and consolidation. The most popular methods of the HEA powder fabrication are mechanical alloying (MA)[117–124] and gas atomizing (GA).[125,126] For the consolidation methods, spark-plasma sintering (SPS),[117,120–123,125,127–131] hot-isostatic pressing (HIP),[118,132] vacuum-hot pressing (VHP),[118] and hot extrusion (HE)[126] have been used to consolidate the HEAs powders. Here, we introduce three manufacturing routes, which are more widely used than others.

1. *MA and SPS*

The "MA + SPS" method could be the most applied fabrication route in the solid-state manufacturing of HEAs. MA is usually accomplished by the ball-milling

Table VIII. Mechanical Properties of HEAs with Different Ni Contents in Various Alloy Systems Refs. [71], [88], [89]

System	Composition	Hardness (HV)	$\sigma_{y,t}$ (MPa)	$\sigma_{max,t}$ (MPa)	$\varepsilon_{p,t}$ (Pct)	Material Preparation Condition	Reference
Al-Co-Cr-Fe-Mo-Ni	$AlCoCrFeMo_{0.5}Ni_0$	904	—	—	—	AC	88
	$AlCoCrFeMo_{0.5}Ni_{1.0}$	770	—	—	—		
	$AlCoCrFeMo_{0.5}Ni_{1.5}$	627	—	—	—		
	$AlCoCrFeMo_{0.5}Ni_{2.0}$	404	—	—	—		
Al-Co-Cr-Fe-Ni	$(AlCoCrFe)_{100}Ni_0$	725	—	—	—	AC	71
	$(AlCoCrFe)_{98.5}Ni_{1.5}$	—	795	1150	3.1		
	$(AlCoCrFe)_{98}Ni_2$	—	680	1130	21.2		
	$(AlCoCrFe)_{97.5}Ni_{2.5}$	—	470	900	25.3		
	$(AlCoCrFe)_{97}Ni_3$	—	387	810	31.2		
	$(AlCoCrFe)_{96}Ni_4$	—	312	660	39		
	$(AlCoCrFe)_{95}Ni_5$	660	—	—	—		
	$(AlCoCrFe)_{90}Ni_{10}$	612	—	—	—		
	$(AlCoCrFe)_{85}Ni_{15}$	616	—	—	—		
	$(AlCoCrFe)_{80}Ni_{20}$	589	—	—	—		
	$(AlCoCrFe)_{72.7}Ni_{27.3}$	583	—	—	—		
	$(AlCoCrFe)_{66.7}Ni_{33.3}$	466	—	—	—		
	$(AlCoCrFe)_{61.5}Ni_{38.5}$	421	—	—	—		
	$(AlCoCrFe)_{57.1}Ni_{42.9}$	406	—	—	—		
	$(AlCoCrFe)_{50}Ni_{50}$	393	—	—	—		
Al-Cr-Fe-Mo-Ni	$AlCrFeMo_{0.2}Ni_{0.5}$	543	—	—	—	AC	89
	$AlCrFeMo_{0.2}Ni_{0.8}$	490	—	—	—		
	$AlCrFeMo_{0.2}Ni_{1.2}$	490	—	—	—		
	$AlCrFeMo_{0.2}Ni_{1.4}$	502	—	—	—		
Co-Cr-Cu-Fe-Ni	$(CoCrCuFe)_{90}Ni_{10}$	170	—	—	—	AC	71
	$(CoCrCuFe)_{85}Ni_{15}$	167	—	—	—		
	$(CoCrCuFe)_{80}Ni_{20}$	157	—	—	—		
	$(CoCrCuFe)_{66.7}Ni_{33.3}$	158	—	—	—		
Co-Cr-Fe-Ni	$(CoCrFe)_{100}Ni_0$	400	—	—	—		
	$(CoCrFe)_{95}Ni_5$	278	—	—	—		
	$(CoCrFe)_{90}Ni_{10}$	196	—	—	—		
	$(CoCrFe)_{85}Ni_{15}$	168	—	—	—		
	$(CoCrFe)_{80}Ni_{20}$	137	—	—	—		
	$(CoCrFe)_{75}Ni_{25}$	134	—	—	—		
	$(CoCrFe)_{60}Ni_{40}$	124	—	—	—		
Co-Fe-Mn-Ni	$(CoFeMn)_{100}Ni_0$	169	—	—	—		
	$(CoFeMn)_{95}Ni_5$	141	—	—	—		
	$(CoFeMn)_{90}Ni_{10}$	144	—	—	—		
	$(CoFeMn)_{85}Ni_{15}$	140	—	—	—		
	$(CoFeMn)_{80}Ni_{20}$	143	—	—	—		
	$(CoFeMn)_{75}Ni_{25}$	144	—	—	—		
	$(CoFeMn)_{60}Ni_{40}$	146	—	—	—		

process. The principal characters of this technology, developed by Benjamin,[133] are the high-energy milling, the omission of the surface-active agent, and the air-sealed condition, which can enable the particles to cold weld with each other. The powders are sintered under a combined effect of the electric current and pressure in the SPS process. The main features of the SPS process consist of a high heating rate, the application of a pressure, and the influence of an electric current.[134]

The HEAs prepared by the "MA + SPS" method show excellent mechanical properties. The hardness can be greatly enhanced, such as the hardness of the CoCrFeNi HEA by the "MA + SPS" technique (570 HV), reported by Praveen *et al.*,[128] is nearly 5 times greater than that by the traditional casting (119 HV).[46] The compressive yield strength and fracture strength can also be greatly increased by the "MA + SPS" method. For example, the compressive yield strength and fracture strength of the CoCrCuFeNi HEA, studied by Wang *et al.*,[135] can be improved from 230 and 888 MPa by traditional casting to 869 and 1865 MPa, using the "MA + SPS" where the yield strength is increased nearly 3 times with a ultimate tensile strain retainment of 32.2 pct. Particularly, as reported by Fu *et al.*,[127] the $Co_{0.5}CrFeNiTi_{0.5}$ HEA fabricated by the "MA + SPS" method exhibits extremely high mechanical properties whose yield stress, compressive strength, compression strain, and hardness are 2.65, 2.69 GPa, 10.0 pct, and 846 HV, respectively.

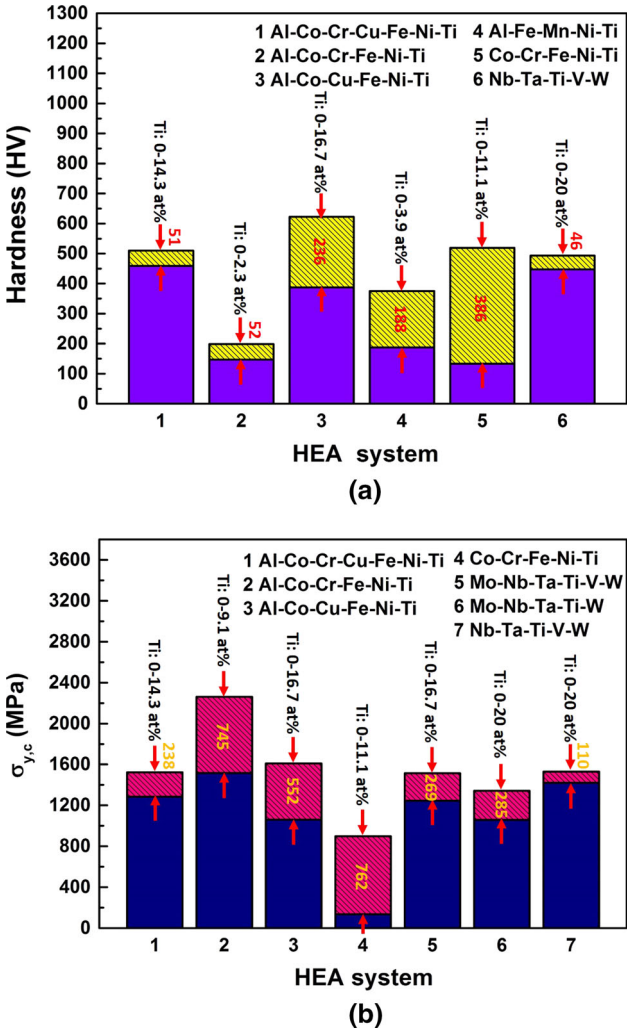

Fig. 12—Values of (*a*) hardnesses of 6 HEA systems[63,72,90–92] and (*b*) compressive yield strengths of 7 HEA systems[72,91–94] with the corresponding Ti-content ranges. The hatched regions are the hardness-change ranges and compressive yield-strength-change ranges of different HEA systems, in (a) and (b), respectively. The colored numbers are the corresponding values of the change ranges (Color figure online).

The reasons behind the enhancement effects of the "MA + SPS" technique can be summarized as nanocrystalline structures, nanoscale twins, and phase transformation. The "MA + SPS" method can introduce ultrafine grains or nanocrystalline phases into HEAs, such as the $CoCr_{0.5-x}CuFeNi_{1.5}V_x$ HEA, studied by Wang *et al.*,[136] which contains ultrafine grains with the sizes between 100 nm and 1 μm. Nanoscale twins are observed in the $Al_{0.6}CoCrFeNiTi_{0.4}$ HEA fabricated by the "MA + SPS" method, and the nanoscale twin boundaries can greatly impede the movement of dislocations, as reported by Fu *et al.*,[129] which will improve the mechanical properties of HEAs. In some HEA systems, there are phase transformations happening during the SPS process. For instance, there is a phase transformation from BCC to σ phases, which is observed by Praveen *et al.*[128] in the temperature range of 500 °C through 600 °C, and the hard σ phase played an important role in the increase of hardness in the CoCrFeNi HEA.

2. *MA and other consolidation methods*

There are some other consolidation methods, except for SPS, which can be used to consolidate the HEAs powder of MA, such as HIP and VHP.

Rogal *et al.*[137] fabricated the CoCrFeMnNi HEA by "MA + HIP," and the compressive yield strength was increased from 230 MPa[96] to 1180 MPa, more than 4 times, compared with the HEA of the same composition by the traditional casting method. Varalakshmi *et al.*[138] used the "MA + VHP" and "MA + HIP" methods, respectively, to fabricate the AlCrCuFeTiZn HEA samples whose hardness can achieve 9.50 and 10.04 GPa (about 969 and 1024 HV). The high hardness and strength of HEAs by "MA + VHP" and "MA + HIP" techniques can also be attributed to the nanocrystalline nature,[138] as well as the large grain-boundary area and the presence of three/two boundaries.[118]

3. *GA and consolidation*

Compared with MA powders, GA powders usually have the higher purity and homogeneity in both the composition and morphology,[125] which enable GA powders to be a good candidate for HEAs manufacturing. The GA powders can be consolidated by SPS, HE, *etc*.

Liu *et al.*[125] studied the CoCrFeMnNi HEA by the "GA + SPS" method with the help of mechanical milling to further refine the microstructures of the GA HEA powders. As they reported, the microstructures of the samples made from the milled GA powders are much finer than those of the ones sintered from the original GA powders. As the milling time became longer, from 4 to 10 hours, the ultimate tensile strength went higher until a certain level, from 762 to 1040 MPa.

The "GA + HE" technique is used by Cai *et al.*[126] to fabricate the $CoCrFeMo_{0.23}Ni$ HEA with great mechanical properties, in which the tensile yield strength, ultimate tensile strength, and elongation are 378, 784 MPa, and 53 pct, respectively. The mechanism behind the strengthening effect can be attributed to the nanocrystalline microstructure[125] and the nano-twins and micro-bands induced during deformation.[126]

IV. DISCUSSION

A. *Elemental Effects*

In order to have a further understanding of the effect of an element, we define a coefficient of hardness as

$$\text{Coefficient} = \frac{\text{Variation of hardness}}{\text{Variation of element atomic percentage} \times 100}. \quad [4]$$

In Eq. [4], the hardness refers to Vickers hardness. With the coefficient, we could have a rough and average

Table IX. Mechanical Properties of HEAs with Different Ti Contents in Various Alloy Systems Refs. [63], [72], [90] through [94]

System	Composition	Hardness (HV)	$\sigma_{y,c}$ (MPa)	$\sigma_{max,c}$ (MPa)	$\varepsilon_{p,c}$ (Pct)	$\sigma_{y,t}$ (MPa)	$\sigma_{max,t}$ (MPa)	$\varepsilon_{p,t}$ (Pct)	Material Preparation Condition	Reference
Al-Co-Cr-Cu-Fe-Ni-Ti	$AlCoCrCuFeNiTi_0$	459	1285	1857	24.6	—	—	—	AC	72
	$AlCoCrCuFeNiTi_{1.0}$	510	1523	1588	8.1	—	—	—		
Al-Co-Cr-Fe-Ni-Ti	$AlCoCrFeNiTi_0$	—	1517	2817	26.9	—	—	—	AC	94
	$AlCoCrFeNiTi_{0.5}$	—	2262	3132	23.2	—	—	—		
	$AlCoCrFeNiTi_{1.0}$	—	1856	2577	8.9	—	—	—		
	$AlCoCrFeNiTi_{1.5}$	—	2220	2718	5.5	—	—	—		
	$Al_{0.3}CoCrFeNiTi_0$	147	—	—	—	—	—	—	ACH, at 973 K	63
	$Al_{0.3}CoCrFeNiTi_{0.1}$	199	—	—	—	—	—	—		
Al-Co-Cu-Fe-Ni-Ti	$AlCoCuFeNiTi_0$	387	1060	1452	19.1	—	—	—	AC	72
	$AlCoCuFeNiTi_{1.0}$	623	1612	1816	12.8	—	—	—		
Al-Fe-Mn-Ni-Ti	$Al_{13}Fe_{36}Mn_{33}Ni_{18}Ti_0$	187	—	—	—	270	578	22.8	ACH, at 823 K or 1,173 K	90
	$Al_{13}Fe_{36}Mn_{33}Ni_{18}Ti_2$	280	—	—	—	532	876	13.9		
	$Al_{13}Fe_{36}Mn_{33}Ni_{18}Ti_4$	375	—	—	—	563	1145	2.3		
Co-Cr-Fe-Ni-Ti	$CoCrFeNiTi_0$	133	136	871	75	—	—	—	AC	91
	$CoCrFeNiTi_{0.3}$	366	648	1529	60	—	—	—		
	$CoCrFeNiTi_{0.5}$	519	898	1502	20	—	—	—		
Mo-Nb-Ta-Ti-V-W	$MoNbTaTi_0VW$	—	1246	1270	1.7	—	—	—	ACH, at 1,473 K	93
	$MoNbTaTi_{1.0}VW$	—	1515	2135	10.6	—	—	—		
Mo-Nb-Ta-Ti-W	$MoNbTaTi_0W$	—	1058	1211	2.6	—	—	—		
	$MoNbTaTi_{1.0}W$	—	1343	2005	14.1	—	—	—		
Nb-Ta-Ti-V-W	$NbTaTi_0VW$	493	1530	1704	12	—	—	—	AC	92
	$NbTaTi_{1.0}VW$	447	1420	1826	20	—	—	—		

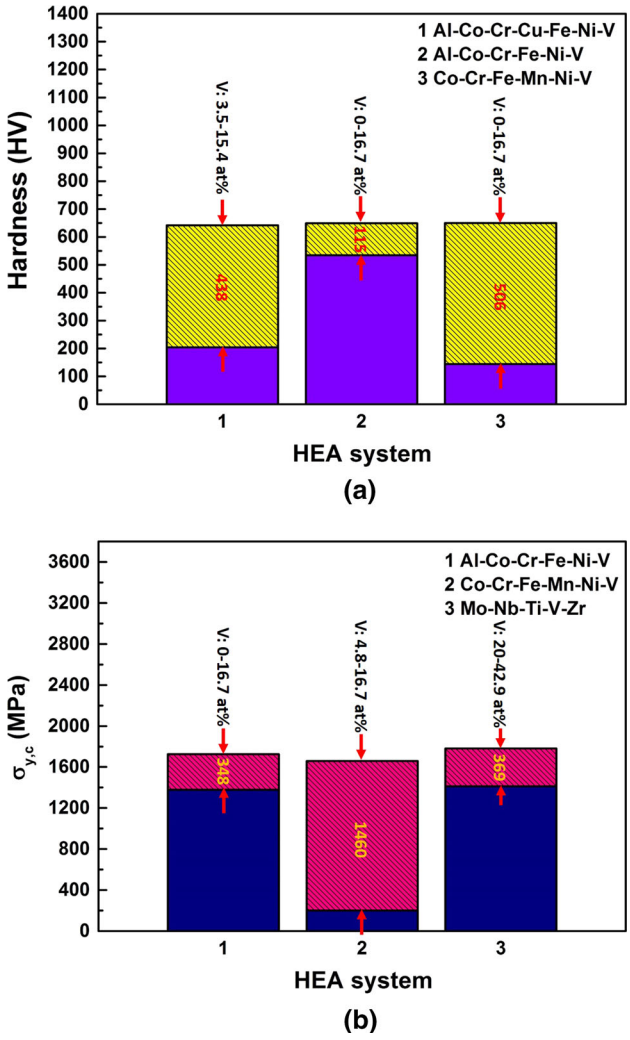

Fig. 13—Values of (*a*) hardnesses of 3 HEA systems[11,77,95] and (*b*) compressive yield strengths of 3 HEA systems[18,77,95] with the corresponding V-content ranges. The hatched regions are the hardness-change ranges and compressive yield-strength-change ranges of different HEA systems, in (a) and (b), respectively. The colored numbers are the corresponding values of the change ranges (Color figure online).

quantification of the influence of each element on the mechanical properties of HEAs.

As shown in Figure 16,[15,16,18–29,31–37,49–56,58–61,66–71,75,77,81,82], we summarized the coefficients of hardness of ten elements in HEAs. The effect of Al should be the most studied element in HEAs, and Al has the largest coefficient range among the HEAs plotted in Figure 16. The coefficient of Al in the Al-Co-Cr-Fe-Ni-Ti HEA system could be as high as 65 HV/100, which means that one percent addition of Al can, on average, improve the hardness by 65 HV. It is worth mentioning that the Al addition can also cause a reduction of strength, such as in the Al-Cr-Fe-Ni-V HEA system,[59] in a certain additional amount. Besides the Al element, Ti, V, and Si could be the other three important elements that will highly strengthen HEAs. The Cr, Mn, and Mo elements will also make contributions to the strengthening behavior in most of HEA systems. The effect of Co could be very small on the mechanical properties of HEAs. Moreover, as increasing the addition of Fe or Ni, there will be a negative effect on the hardness of HEAs in most of the reported HEA systems.

Fe, Ni, Co, and Cr could be the four most common principal elements in HEAs. It is worth noting that Fe, Ni, Co, and Cr have similar atomic radii, which seems to render similar lattice distortions accompanying with their strengthening effects. However, Fe and Ni elements can have negative effect on the hardness, while Cr is thought to have positive effects, and Co shows insignificant effects in HEAs. The main reason for the above phenomenon could be that the traditional lattice-distortion mechanism is developed to explain the lattice distortion in traditional crystal materials with non-distorted lattice matrix rather than in HEAs. The traditional lattice-distortion mechanism will be not suitable for HEAs, which have the lattice distortion as their intrinsic feature. Therefore, the new lattice-distortion strengthening mechanism for HEAs needs to be further investigated. However, Fe, Ni, Co, and Cr are still the important ingredients in HEAs, which are also mostly studied. One reason for this trend is their wide use in industrial applications and good accessibility. Another reason could be their similar atomic radii, which are required in forming solid-solution phases. In the formation rules of solid-solution phase in HEAs proposed by Zhang *et al.*[8], there is a Δ parameter used to predict the phase formation, which is described as follows:

$$\Delta = \sqrt{\sum_{i=1}^{N} c_i(1 - r_i/\overline{r})^2}. \qquad [5]$$

In Eq. [5], the N represents the number of elements in the alloy; c_i and r_i represent the atomic percentage and atomic radius of the ith element, respectively; $\overline{r}$ is the average atomic radius of the elements in the alloy. For the alloys with small difference of atomic radii, their values of the Δ parameter will be low. Regarding the HEAs, their values (less than 6) are relatively lower than those of the bulk metallic glass (large than 6). Therefore, the Fe, Ni, Co, and Cr play important roles in the HEAs.

The influence of elemental strengthening on mechanical properties could be mainly attributed to solid-solution strengthening and phase transformations. The solid-solution strengthening should be the most primary strengthening mechanism of the elemental enhancement of HEAs corresponding to the nature of severe lattice

Table X. Mechanical Properties of HEAs with Different V Contents in Various Alloy Systems Refs. [11], [18], [77], [95], [142]

System	Composition	Hardness (HV)	$\sigma_{y,c}$ (MPa)	$\sigma_{max,c}$ (MPa)	$\varepsilon_{p,c}$ (Pct)	$\sigma_{y,t}$ (MPa)	$\sigma_{max,t}$ (MPa)	$\varepsilon_{p,t}$ (Pct)	Material Preparation Condition	Reference
Al-Co-Cr-Cu-Fe-Ni-V	$Al_{0.5}CoCrCuFeNiV_0$	223	—	—	—	—	—	—	AC	11
	$Al_{0.5}CoCrCuFeNiV_{0.2}$	204	—	—	—	—	—	—		
	$Al_{0.5}CoCrCuFeNiV_{0.4}$	231	—	—	—	—	—	—		
	$Al_{0.5}CoCrCuFeNiV_{0.6}$	331	—	—	—	—	—	—		
	$Al_{0.5}CoCrCuFeNiV_{0.8}$	451	—	—	—	—	—	—		
	$Al_{0.5}CoCrCuFeNiV_{1.0}$	642	—	—	—	—	—	—		
	$Al_{0.5}CoCrCuFeNiV_{1.2}$	578	—	—	—	—	—	—		
	$Al_{0.5}CoCrCuFeNiV_{1.4}$	579	—	—	—	—	—	—		
	$Al_{0.5}CoCrCuFeNiV_{1.6}$	598	—	—	—	—	—	—		
	$Al_{0.5}CoCrCuFeNiV_{1.8}$	601	—	—	—	—	—	—		
	$Al_{0.5}CoCrCuFeNiV_{2.0}$	590	—	—	—	—	—	—		
Al-Co-Cr-Fe-Ni-V	$AlCoCrFeNiV_0$	534	1379	2865	22.7	—	—	—	AC	95
	$AlCoCrFeNiV_{0.2}$	558	1492	3298	26.8	—	—	—		
	$AlCoCrFeNiV_{0.5}$	591	1598	1907	5.1	—	—	—		
	$AlCoCrFeNiV_{0.8}$	625	1695	2097	5.7	—	—	—		
	$AlCoCrFeNiV_{1.0}$	649	1727	1867	0.7	—	—	—		
Co-Cr-Fe-Mn-Ni-V	$CoCrFeMnNiV_0$	144	230	—	—	215	491	71	AC or ACH, at 1273 K	77
	$CoCrFeMnNiV_{0.25}$	151	200	—	—	—	—	—		
	$CoCrFeMnNiV_{0.5}$	186	620	—	—	—	—	—		
	$CoCrFeMnNiV_{0.75}$	342	740	1325	7.8	—	—	—		
	$CoCrFeMnNiV_{1.0}$	650	1660	1845	0.5	—	90	0		
Cr-Fe-Ti-V-Zr	$Cr_{10}Fe_{15}Ti_{35}V_{35}Zr_5$	—	918	1013	0.7	—	—	—	AC	142
Mo-Nb-Ti-V-Zr	$MoNbTiV_0Zr$	—	1575	3477	33.4	—	—	—	ABS	18
	$MoNbTiV_{0.25}Zr$	—	1767	3875	30.1	—	—	—		
	$MoNbTiV_{0.5}Zr$	—	1642	3295	28	—	—	—		
	$MoNbTiV_{0.75}Zr$	—	1686	3920	29.3	—	—	—		
	$MoNbTiV_{1.0}Zr$	—	1782	3818	25.8	—	—	—		
	$MoNbTiV_{1.5}Zr$	—	1435	3305	20	—	—	—		
	$MoNbTiV_{2.0}Zr$	—	1524	3174	23.1	—	—	—		
	$MoNbTiV_{3.0}Zr$	—	1413	2507	23.6	—	—	—		

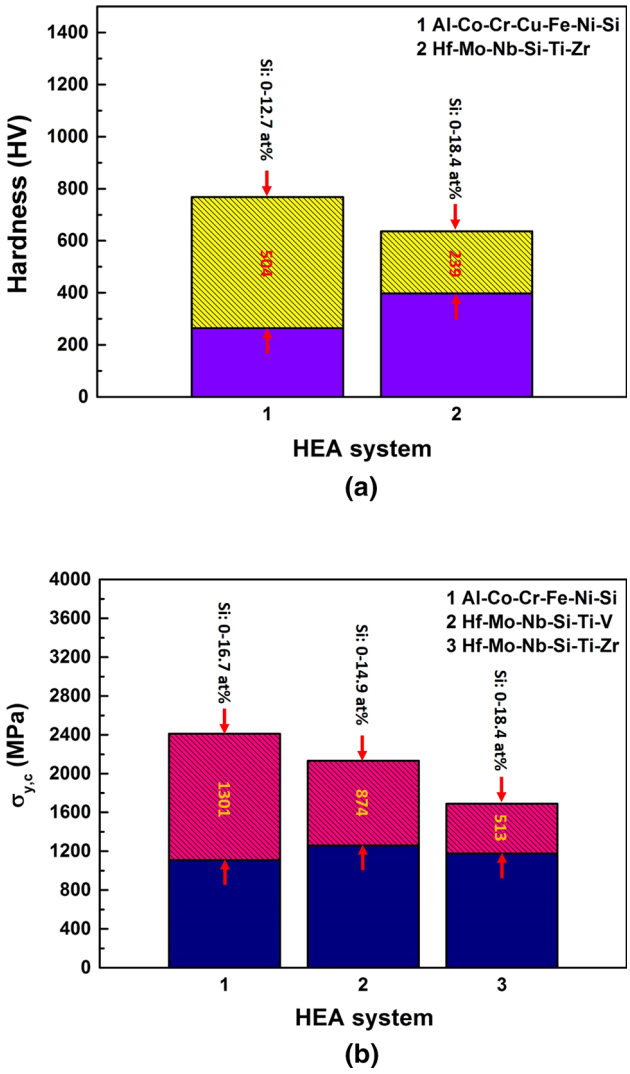

Fig. 14—Values of (*a*) hardnesses of 2 HEA systems[99,100] and (*b*) compressive yield strengths of 3 HEA systems[27,100,101] with the corresponding Si-content ranges. The hatched regions are the hardness-change ranges and compressive yield-strength-change ranges of different HEA systems, in (a) and (b), respectively. The colored numbers are the corresponding values of the change ranges (Color figure online).

distortion. The phase transformations mainly refer to the increase of hard phases, such as BCC, σ, and Laves phases.

B. *Effects of Fabrication Methods*

As shown in Figure 17,[108,114,122,125–127,129,130,135,137,139–141], the HEAs fabricated by the "MA + consolidation" method exhibit much higher strength than the HEAs produced using other methods. On the aspect of plasticity, the HEAs by the "GA + consolidation" technique have an advantage, compared with the AM, BS, and "MA + consolidation" methods.

For the specific HEA, such as the CoCrFeMnNi HEA, the tensile yield strength and plasticity by the "MA + consolidation" and "GA + consolidation" techniques are 1180 MPa, 35.5 pct,[137] and 312 MPa, 27 pct,[141] respectively, while those of the HEA in the as-cast state are 211 MPa and 61.7 pct.[49] The former two methods show the great strengthening effect on the yield strength of the HEA, especially the "MA + consolidation," which can improve the yield strength by more than 4 times, compared with the traditional method of melting and casting. It is worth mentioning that the "GA + consolidation" with the help of the ball-milling process can enable the tensile strength of the CoCrFeMnNi HEA to reach as high as 1000 MPa.[125]

The main reason for the enhancement of the "MA + consolidation" and "GA + consolidation" techniques should be the introduction of ultrafine grains *via* the fabrication process. In this respect, the grain size of MA powders can be reduced to sizes on the order of a nanometer, which is much smaller than that of GA powders as well as other HEAs made by different methods. In addition, the consolidation technologies can also influence the grain size because of their different heating rates. Among the consolidation methods, SPS has the highest heating rate, which will give less time for grain growth. By this token, the combination of MA and SPS should be the preferable fabrication route than others.

Therefore, in general, the order of choice of the manufacturing method for strengthening should be the "MA + consolidation," "GA + consolidation," and "Melting + casting" methods.

However, for the purposes of promoting plasticity, the method of the "melting and casting" could have the advantage over the solid-state technique, such as the "MA + consolidation" or "GA + consolidation" methods. Especially, the Bridgman solidification could be the best approach to improve the plasticity of HEAs.

V. FUTURE DIRECTIONS

The reported mechanical behavior of HEAs mainly focuses on the hardness and compressive properties, while the tensile behavior, which is very important for industrial applications, was studied and reported less than the former two properties. Furthermore, the creep and fatigue properties are much less investigated than the three properties listed above. The research of mechanical behavior still needs to be continued for future applications.

It is an effective way to strengthen the mechanical properties of HEAs by adding elements as minor components without being restricted to the equiatomic

Table XI. Mechanical Properties of HEAs with Different Si Contents in Various Alloy Systems Refs. [27], [99] through [101]

System	Composition	Hardness (HV)	$\sigma_{y,c}$ (MPa)	$\sigma_{max,c}$ (MPa)	$\varepsilon_{p,c}$ (Pct)	Material Preparation Condition	References
Al-Co-Cr-Cu-Fe-Ni-Si	$Al_{0.5}CoCrCuFeNiSi_0$	264	—	1260	> 30	AC	99
	$Al_{0.5}CoCrCuFeNiSi_{0.4}$	435	—	1790	23		
	$Al_{0.5}CoCrCuFeNiSi_{0.8}$	768	—	1060	0		
Al-Co-Cr-Fe-Ni-Si	$AlCoCrFeNiSi_0$	—	1110	—	—	AIIC	101
	$AlCoCrFeNiSi_{0.2}$	—	1265	2173	13.8		
	$AlCoCrFeNiSi_{0.4}$	—	1481	2444	13.4		
	$AlCoCrFeNiSi_{0.6}$	—	1834	2195	2.6		
	$AlCoCrFeNiSi_{0.8}$	—	2179	2664	1.8		
	$AlCoCrFeNiSi_{1.0}$	—	2411	2950	1.2		
Hf-Mo-Nb-Si-Ti-V	$HfMo_{0.5}NbSi_0TiV_{0.5}$	—	1260	—	> 35	IC	27
	$HfMo_{0.5}NbSi_{0.3}TiV_{0.5}$	—	1617	2016	18.5		
	$HfMo_{0.5}NbSi_{0.5}TiV_{0.5}$	—	1787	2052	11.9		
	$HfMo_{0.5}NbSi_{0.7}TiV_{0.5}$	—	2134	2242	9.2		
Hf-Mo-Nb-Si-Ti-Zr	$Hf_{0.5}Mo_{0.5}NbSi_0TiZr$	398	1177	1526	24.7	AC	100
	$Hf_{0.5}Mo_{0.5}NbSi_{0.1}TiZr$	441	1368	2101	27.8		
	$Hf_{0.5}Mo_{0.5}NbSi_{0.3}TiZr$	494	1430	2047	23.2		
	$Hf_{0.5}Mo_{0.5}NbSi_{0.5}TiZr$	523	1604	1946	22.7		
	$Hf_{0.5}Mo_{0.5}NbSi_{0.7}TiZr$	581	1614	1928	12.3		
	$Hf_{0.5}Mo_{0.5}NbSi_{0.9}TiZr$	637	1690	2024	9.1		

compositions. Non-equiatomic HEAs with the great mechanical behavior in normal or extreme conditions can be expected in the future.

Unlike the traditional materials, such as steels and aluminum alloys, which have one major element and certain naming rules, HEAs, which have several major elements, do not have particular widely accepted naming rules. For example, the display order of the composition of HEAs could follow the alphabet or the periodic table of elements. For example, the HEA with the equiatomic composition of Al, Co, Cr, Fe, and Ni, can be named as AlCrFeCoNi, following the periodic table or AlCoCrFeNi, following the alphabet order. Nowadays, the alphabetical ordering scheme seems more widely used than others. It will be more convenient for researchers if we can establish a widely accepted naming rule.

The solid-state manufacturing techniques show great strengthening effects on the mechanical properties of HEAs, especially the "MA + consolidation" method. It can be used to improve the HEAs with the low strength and high plasticity, such as most of the FCC HEAs, to achieve outstanding comprehensive mechanical properties. Importantly, this technique can also be employed to fabricate the refractory HEAs, which are hard to achieve high homogeneity, without segregation, by arc-melting and casting. We can expect the industrial applications of the HEAs by solid-state manufacturing in the near future.

The AM, as a novel manufacturing method, is still in the early stage concerning the area of HEAs. The future of AM on industrial applications is very bright for its features of time and material saving, as well as making free shapes. There should be more intensive research on HEAs by AM.

Moreover, since most of the solid-state manufacturing and AM technologies required HEAs powders as prefabricated materials, more research on manufacturing high-quality HEAs powders is needed in the future, which will promote the applications of HEAs.

Except for the applications that involve small loading and compressive loading, room-temperature structural applications would require a good combination of strength and ductility (or toughness). Those strengthening mechanisms, such as solution hardening, precipitation hardening, grain-size hardening, nano-twinning deformation, and strain-induced phase transformations common in traditional alloys would also be pursued in HEAs. Evidence of the benefits resulting from these factors has been observed in experiments of HEAs. Therefore, how to design compositions and processes

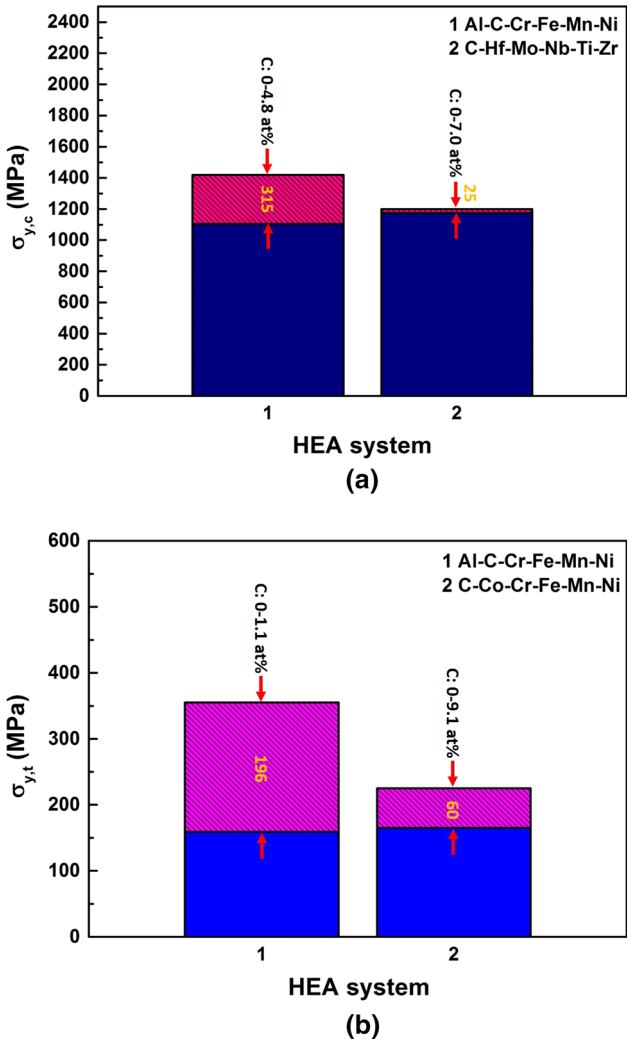

Fig. 15—Values of (*a*) compressive yield strengths of 2 HEA systems[102,103] and (*b*) tensile yield strengths of 2 HEA systems[104–106] with the corresponding C-content ranges. The hatched regions are the compressive and tensile yield-strength-change ranges of different HEA systems, in (a) and (b), respectively. The colored numbers are the corresponding values of the change ranges (Color figure online).

for fully utilizing the mechanisms and optimizing the combination of properties is still an important issue in the future.

VI. CONCLUSIONS

This paper reviewed the two aspects, *i.e.*, constituent elements and manufacturing methods, which influence the mechanical properties of HEAs. As we discussed above, they can result in large variations in the hardness, strength, and ductility, which is mainly related to the structural applications. This trend demonstrates that the composition and process design still have a large space to be optimized for the excellent property combination.

Based on the reported research, the elemental effect can be different, *i.e.*, positive or negative, on the strength of HEAs. For example, Fe and Ni could be typical negative-effect elements, which will decrease the strength of HEAs, while Mo, V, and Si have positive effects in most circumstances. It is worth mentioning that the effects of the same element could be opposite in different HEA systems. For instance, the Al element will improve the strength in most HEA systems but have negative effects on the Al-Cr-Fe-Ni-V HEA system[59] within a certain addition amount. The solid-solution strengthening, phase transformation, and phase distribution and morphology could be the main three pathways of the elemental effects on HEAs strengthening behaviors. Al, Ti, Si, and V could be the four most powerful elements for strengthening HEAs.

Besides the melting and casting method, "MA + consolidation," "GA + consolidation," BS and AM techniques are widely used to fabricate HEAs. The HEAs fabricated by the methods of the "MA + consolidation," "GA + consolidation," and AM methods can possess the ultrafine grain, which will make an improvement of the strength of HEAs. The "MA + consolidation" technique could be the most effective method to improve the strength of HEAs.

Moreover, AM, as a novel manufacturing method, has been used to fabricate HEAs with good mechanical properties, comparable with traditional methods. The

Table XII. Mechanical Properties of HEAs with Different C Contents in Various Alloy Systems Refs. [102] through [107]

System	Composition	Hardness (HV)	$\sigma_{y,c}$ (MPa)	$\sigma_{max,c}$ (MPa)	$\varepsilon_{p,c}$ (Pct)	$\sigma_{y,t}$ (MPa)	$\sigma_{max,t}$ (MPa)	$\varepsilon_{p,t}$ (Pct)	Material Preparation Condition	Reference
Al-C-Cr-Fe-Mn-Ni	$AlC_0CrFeMnNi$	—	1420	2613	24.8	—	—	—	IC	103
	$AlC_{0.08}CrFeMnNi$	—	1297	2959	30.6	—	—	—		
	$AlC_{0.17}CrFeMnNi$	—	1338	2482	25.2	—	—	—		
	$AlC_{0.25}CrFeMnNi$	—	1105	2931	27.8	—	—	—		
	$Al_{7.5}C_0Cr_6Fe_{40.4}Mn_{34.8}Ni_{11.3}$	—	—	—	—	159	535	40.8	AC	104
	$Al_{7.20}C_{0.07}Cr_{5.52}Fe_{41.83}Mn_{35.25}Ni_{10.13}$	—	—	—	—	171	674	51.6		
	$Al_{7.10}C_{0.16}Cr_{5.01}Fe_{40.6}Mn_{35.55}Ni_{11.58}$	—	—	—	—	181	713	52.2		
	$Al_{7.35}C_{0.30}Cr_{5.20}Fe_{44.85}Mn_{32.25}Ni_{10.05}$	—	—	—	—	208	762	48.2		
	$Al_{7.39}C_{0.55}Cr_{5.31}Fe_{41.08}Mn_{35.46}Ni_{10.21}$	—	—	—	—	274	960	52.3		
	$Al_{7.40}C_{1.1}Cr_{5.55}Fe_{39.93}Mn_{35.67}Ni_{10.35}$	—	—	—	—	355	1174	49.5		
C-Co-Cr-Fe-Mn-Ni	$C_0CoCrFeMnNi$	160	—	—	—	165	520	65	AC or ACHRH	106, 107
	$C_{0.1}CoCrFeMnNi$	204	—	—	—	—	—	—		
	$C_{0.175}CoCrFeMnNi$	240	—	—	—	—	—	—		
	$C_{0.25}CoCrFeMnNi$	275	—	—	—	—	—	—		
	$C_{0.5}CoCrFeMnNi$	—	—	—	—	225	655	38	ACHRH	105
C-Hf-Mo-Nb-Ti-Zr	$C_0Hf_{0.5}Mo_{0.5}NbTiZr$	—	1176	1538	24.6	—	—	—	AC	102
	$C_{0.1}Hf_{0.5}Mo_{0.5}NbTiZr$	—	1183	2139	38.4	—	—	—		
	$C_{0.3}Hf_{0.5}Mo_{0.5}NbTiZr$	—	1201	1965	32.6	—	—	—		

$\sigma_{y,c}$, compressive yield strength; $\sigma_{max,c}$, ultimate compressive strength; $\varepsilon_{p,c}$, ultimate compressive strain; $\sigma_{y,t}$, tensile yield strength; $\sigma_{max,t}$, ultimate tensile strength; $\varepsilon_{p,t}$, ultimate tensile strain.

AIIC, arc-melting and casting + induction-melting and injection-casting; AC, arc-melting and casting; IC, induction-melting and casting; ACH, arc-melting and casting + heat-treatment; ACR, arc-melting and casting + cold-rolling; ACHIP, arc-melting and casting + hot-isostatic-pressing; MC, melting and casting; ABS, arc-melting and casting + Bridgman solidification.

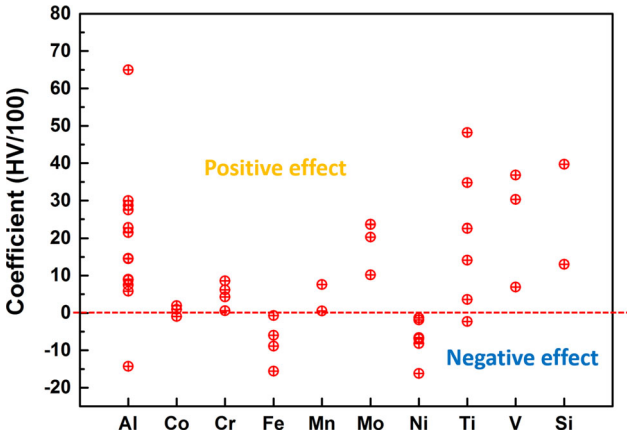

Fig. 16—The distribution of hardnesses coefficients of 10 elements in HEAs.[15,16,18–29,31–37,49–56,58–61,66–71,75,77,81,82]

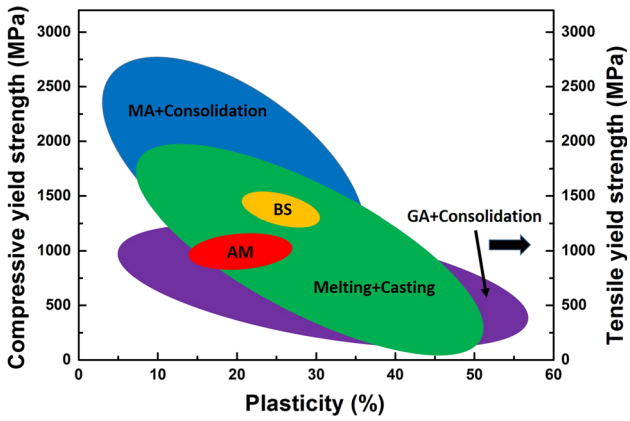

Fig. 17—The summary of compressive/tensile yield strength *vs.* plasticity of HEAs fabricated by different manufacturing methods,[108,114,122,125–127,129,130,135,137,139–141] in which the yield strengths of HEAs by "GA + Consolidation" refer to the tensile yield strengths while the rest are compressive yield strengths.

features of AM, such as the short fabrication time, materials saving, and the ability to achieve complex shapes of products, will give HEAs a bright future in industrial applications.

ACKNOWLEDGMENTS

PKL would like to acknowledge the Department of Energy (DOE), Office of Fossil Energy, National Energy Technology Laboratory (DE-FE-0008855, DE-FE-0024054), with Mr. V. Cedro and Mr. R. Dunst as program managers. ZL and PKL acknowledge the support from the Project of DE-FE-0011194 with the program manager, Dr. J. Mullen. PKL very much appreciates the support of the U.S. Army Research Office Project (W911NF-13-1-0438) with the program managers, Dr. M.P. Bakas and Dr. D.M. Stepp. PKL acknowledges the support from the National Science Foundation (DMR-1611180 and 1809640) with the program directors, Drs. G. Shiflet and D. Farkas. PKL would like to thank QuesTek Innovations, LLC (QuesTek) under the Award of No. DE-SC0013220 with Dr. J. Saal as the program manager. PKL is pleased to acknowledge the financial support by the Ministry of Science and Technology of Taiwan, under Grant No. of MOST 105-2221-E-007-017-MY3, and the Department of Materials Science and Engineering, National Tsing Hua University, Taiwan. The authors very much appreciate the support of the Center for Materials Processing with Professor Claudia Rawn as the director. ZL very much appreciates the efforts of Mr. James Brechtl for grammar checking.

REFERENCES

1. J.W. Yeh, S.K. Chen, S.J. Lin, J.Y. Gan, T.S. Chin, T.T. Shun, C.H. Tsau, and S.Y. Chang: *Adv. Eng. Mater.*, 2004, vol. 6, pp. 299–03.
2. B.S. Murty, J.W. Yeh, and S. Ranganathan: *High-Entropy Alloys*, Butterworth-Heinemann, Oxford, 2014.
3. B. Cantor, I.T.H. Chang, P. Knight, and A.J.B. Vincent: *Mater. Sci. Eng. A*, 2004, vols. 375–377, pp. 213–18.
4. S. Ranganathan: *Curr. Sci.*, 2003, vol. 85, pp. 1404–06.
5. J.W. Yeh: *JOM*, 2013, vol. 65, pp. 1759–71.
6. D.B. Miracle and O.N. Senkov: *Acta Mater.*, 2017, vol. 122, pp. 448–11.
7. H.Y. Diao, R. Feng, K.A. Dahmen, and P.K. Liaw: *Curr. Opin. Solid State Mater. Sci.*, 2017, vol. 21, pp. 252–66.
8. Y. Zhang, Y.J. Zhou, J.P. Lin, G.L. Chen, and P.K. Liaw: *Adv. Eng. Mater.*, 2008, vol. 10, pp. 534–38.
9. L.J. Santodonato, Y. Zhang, M. Feygenson, C.M. Parish, M.C. Gao, R.J. Weber, J.C. Neuefeind, Z. Tang, and P.K. Liaw: *Nat. Commun.*, 2015, vol. 6, p. 5964.
10. M.C. Gao, J.W. Yeh, P.K. Liaw, and Y. Zhang: *High-Entropy Alloys: Fundamentals and Applications*, Springer, Basel, 2016.
11. M.-R. Chen, S.-J. Lin, J.-W. Yeh, S.-K. Chen, Y.-S. Huang, and M.-H. Chuang: *Metall. Mater. Trans. A*, 2006, vol. 37A, pp. 1363–69.
12. W. Jien-Min, S.-J. Lin, J.-W. Yeh, S.-K. Chen, Y.-S. Huang, and H.-C. Chen: *Wear*, 2006, vol. 261, pp. 513–19.
13. C.-C. Tung, J.-W. Yeh, T.-t. Shun, S.-K. Chen, Y.-S. Huang, and H.-C. Chen: *Mater. Lett.*, 2007, vol. 61, pp. 1–5.
14. S. Varalakshmi, M. Kamaraj, and B.S. Murty: *J. Alloy. Compd.*, 2008, vol. 460, pp. 253–57.
15. C.-W. Tsai, Y.-L. Chen, M.-H. Tsai, J.-W. Yeh, T.-T. Shun, and S.-K. Chen: *J. Alloy. Compd.*, 2009, vol. 486, pp. 427–35.
16. C.-Y. Hsu, C.-C. Juan, W.-R. Wang, T.-S. Sheu, J.-W. Yeh, and S.-K. Chen: *Mater. Sci. Eng. A*, 2011, vol. 528, pp. 3581–88.
17. M.A. Hemphill, T. Yuan, G.Y. Wang, J.W. Yeh, C.W. Tsai, A. Chuang, and P.K. Liaw: *Acta Mater.*, 2012, vol. 60, pp. 5723–34.
18. Y. Zhang, X. Yang, and P.K. Liaw: *JOM*, 2012, vol. 64, pp. 830–38.
19. B. Gludovatz, A. Hohenwarter, D. Catoor, E.H. Chang, E.P. George, and R.O. Ritchie: *Science*, 2014, vol. 345, pp. 1153–58.
20. S. Liu, M.C. Gao, P.K. Liaw, and Y. Zhang: *J. Alloy. Compd.*, 2015, vol. 619, pp. 610–15.
21. F. Meng and I. Baker: *J. Alloy. Compd.*, 2015, vol. 645, pp. 376–81.
22. O.N. Senkov, J.D. Miller, D.B. Miracle, and C. Woodward: *Nature communications*, 2015, vol. 6, p. 6529.
23. J.Y. He, C. Zhu, D.Q. Zhou, W.H. Liu, T.G. Nieh, and Z.P. Lu: *Intermetallics*, 2014, vol. 55, pp. 9–14.
24. R. Carroll, C. Lee, C.W. Tsai, J.W. Yeh, J. Antonaglia, B.A. Brinkman, M. LeBlanc, X. Xie, S. Chen, P.K. Liaw, and K.A. Dahmen: *Scientific reports*, 2015, vol. 5, p. 16997.

25. H. Huang, Y. Wu, J. He, H. Wang, X. Liu, K. An, W. Wu, and Z. Lu: *Adv. mater.*, 2017, vol. 17, pp. 1–7.
26. T.K. Liu, Z. Wu, A.D. Stoica, Q. Xie, W. Wu, Y.F. Gao, H. Bei, and K. An: *Mater. Des.*, 2017, vol. 131, pp. 419–27.
27. Y. Liu, Y. Zhang, H. Zhang, N. Wang, X. Chen, H. Zhang, and Y. Li: *J. Alloy. Compd.*, 2017, vol. 694, pp. 869–76.
28. Y.H. Zhang, Y. Zhuang, A. Hu, J.J. Kai, and C.T. Liu: *Scripta Mater.*, 2017, vol. 130, pp. 96–99.
29. O.N. Senkov, G.B. Wilks, D.B. Miracle, C.P. Chuang, and P.K. Liaw: *Intermetallics*, 2010, vol. 18, pp. 1758–65.
30. K.M. Youssef, A.J. Zaddach, C. Niu, D.L. Irving, and C.C. Koch: *Mater. Res. Lett.*, 2014, vol. 3, pp. 95–99.
31. Z. Tang, T. Yuan, C.-W. Tsai, and J.-W. Yeh: *Acta Mater.*, 2015, vol. 99, pp. 247–58.
32. M.-H. Tsai and J.-W. Yeh: *Mater. Res. Lett.*, 2014, vol. 2, pp. 107–23.
33. A.T. Samaei, M.M. Mirsayar, and M.R.M. Aliha: *Eng. Solid Mech.*, 2015, vol. 3, pp. 1–20.
34. Y. Zhang, T.T. Zuo, Z. Tang, M.C. Gao, K.A. Dahmen, P.K. Liaw, and Z.P. Lu: *Prog Mater Sci*, 2014, vol. 61, pp. 1–93.
35. M.-H. Tsai: *Entropy*, 2013, vol. 15, pp. 5338–45.
36. E.J. Pickering and N.G. Jones: *Int. Mater. Rev.*, 2016, vol. 61, pp. 183–202.
37. Y. Shi, B. Yang, and P.K. Liaw: *Metals*, 2017, vol. 7, p. 43.
38. Z.P. Lu, H. Wang, M.W. Chen, I. Baker, J.W. Yeh, C.T. Liu, and T.G. Nieh: *Intermetallics*, 2015, vol. 66, pp. 67–76.
39. W. Li, P. Liu, and P.K. Liaw: *Mater. Res. Lett.*, 2018, vol. 6, pp. 199–29.
40. I. Baker, M. Wu, and Z. Wang: *Mater. Charact.*, 2018, https://doi.org/10.1016/j.matchar.2018.07.030.
41. M. Widom: *J. Mater. Res.*, 2018, https://doi.org/10.1557/jmr.2018.222.
42. Z. Lyu, X. Fan, C. Lee, S.-Y. Wang, R. Feng, and P.K. Liaw: *J. Mater. Res.*, 2018, https://doi.org/10.1557/jmr.2018.273.
43. S. Praveen and H.S. Kim: *Adv. Eng. Mater.*, 2018, vol. 20, p. 1700645.
44. S. Huang, F. Tian and L. Vitos, *Journal of Materials Research* 2018, pp. 1–16.
45. L. Ma, C. Li, Y. Jiang, L. Jinlian Zhou, F.W. Wang, T. Cao, and Y. Xue: *J. Alloy. Compd.*, 2017, vol. 694, pp. 61–67.
46. W.-R. Wang, W.-L. Wang, S.-C. Wang, Y.-C. Tsai, C.-H. Lai, and J.-W. Yeh: *Intermetallics*, 2012, vol. 26, pp. 44–51.
47. O.N. Senkov, C. Woodward, and D.B. Miracle: *JOM*, 2014, vol. 66, pp. 2030–42.
48. H.F. Sun, C.M. Wang, X. Zhang, R.Z. Li, and L.Y. Ruan: *Mater. Res. Innov.*, 2015, vol. 19, pp. S8-89–S8-93.
49. J.Y. He, W.H. Liu, H. Wang, Y. Wu, X.J. Liu, T.G. Nieh, and Z.P. Lu: *Acta Mater.*, 2014, vol. 62, pp. 105–13.
50. S. Guo, C. Ng, and C.T. Liu: *J. Alloys Compd*, 2013, vol. 557, pp. 77–81.
51. M.-H. Chuang, M.-H. Tsai, W.-R. Wang, S.-J. Lin, and J.-W. Yeh: *Acta Mater.*, 2011, vol. 59, pp. 6308–17.
52. J.-W. Yeh, S.-K. Chen, J.-Y. Gan, S.-J. Lin, T.-S. Chin, T.-T. Shun, C.-H. Tsau, and S.-Y. Chang: *Metall. Mater. Trans. A*, 2004, vol. 35A, pp. 2533–36.
53. H.M. Daoud, A. Manzoni, R. Völkl, N. Wanderka, and U. Glatzel: *JOM*, 2013, vol. 65, pp. 1805–14.
54. B.-y. Li, K. Peng, H. Ai-ping, L.-p. Zhou, J.-j. Zhu, and D.-y. Li: *Trans. Nonferrous Metals Soc. China*, 2013, vol. 23, pp. 735–41.
55. T.-T. Shun and D. Yu-Chin: *J. Alloy. Compd.*, 2009, vol. 479, pp. 157–60.
56. C. Li, J.C. Li, M. Zhao, and Q. Jiang: *J. Alloy. Compd.*, 2010, vol. 504, pp. S515–18.
57. S.G. Ma, Z.D. Chen, and Y. Zhang: *Mater. Sci. Forum*, 2013, vols. 745–746, pp. 706–14.
58. S.-T. Chen, W.-Y. Tang, Y.-F. Kuo, S.-Y. Chen, C.-H. Tsau, T.-T. Shun, and J.-W. Yeh: *Mater. Sci. Eng. A*, 2010, vol. 527, pp. 5818–25.
59. S. Xia, X. Yang, M. Chen, T. Yang, and Y. Zhang: *Metals*, 2017, vol. 7, p. 18.
60. N. Yu Yurchenko, N.D. Stepanov, D.G. Shaysultanov, M.A. Tikhonovsky, and G.A. Salishchev: *Mater. Charact.*, 2016, vol. 121, pp. 125–34.
61. N.D. Stepanov, N. Yu Yurchenko, D.G. Shaysultanov, G.A. Salishchev, and M.A. Tikhonovsky: *Mater. Sci. Technol.*, 2015, vol. 31, pp. 1184–93.
62. C.-Y. Hsu, C.-C. Juan, T.-S. Sheu, S.-K. Chen, and J.-W. Yeh: *JOM*, 2013, vol. 65, pp. 1840–47.
63. T.-T. Shun, C.-H. Hung, and C.-F. Lee: *J. Alloy. Compd.*, 2010, vol. 495, pp. 55–58.
64. Y. Zhang, T. Zuo, Y. Cheng, and P.K. Liaw: *Sci. Rep.*, 2013, vol. 3, p. 1455.
65. Y.J. Zhou, Y. Zhang, Y.L. Wang, and G.L. Chen: *Mater. Sci. Eng., A*, 2007, vols. 454–455, pp. 260–65.
66. Y.J. Zhou, Y. Zhang, F.J. Wang, and G.L. Chen: *Appl. Phys. Lett.*, 2008, vol. 92, p. 241917.
67. F.J. Wang, Y. Zhang, and G.L. Chen: *J. Alloy. Compd.*, 2009, vol. 478, pp. 321–24.
68. K.B. Zhang, Z.Y. Fu, J.Y. Zhang, W.M. Wang, H. Wang, Y.C. Wang, Q.J. Zhang, and J. Shi: *Mater. Sci. Eng., A*, 2009, vol. 508, pp. 214–19.
69. Z. Tang, M.C. Gao, H.y. Diao, T. Yang, J. Liu, T. Zuo, Y. Zhang, L. Zhaoping, Y. Cheng, Y. Zhang, K.A. Dahmen, P.K. Liaw, and T. Egami: *JOM*, 2013, vol. 65, pp. 1848–58.
70. X.Y. Gao, N. Liu, Y.X. Jin, and Z.X. Zhu: *Mater. Sci. Forum*, 2014, vol. 789, pp. 79–83.
71. Z.G. Zhu, K.H. Ma, Q. Wang, and C.H. Shek: *Intermetallics*, 2016, vol. 79, pp. 1–11.
72. D.H. Xiao, P.F. Zhou, W.Q. Wu, H.Y. Diao, M.C. Gao, M. Song, and P.K. Liaw: *Mater. Des.*, 2017, vol. 116, pp. 438–47.
73. N.D. Stepanov, N. Yu Yurchenko, D.V. Skibin, M.A. Tikhonovsky, and G.A. Salishchev: *J. Alloy. Compd.*, 2015, vol. 652, pp. 266–80.
74. N.D. Stepanov, D.G. Shaysultanov, M.A. Tikhonovsky, and G.A. Salishchev: *Mater. Des.*, 2015, vol. 87, pp. 60–65.
75. C.-F. Lee and T.-T. Shun: *Mater. Charact.*, 2016, vol. 114, pp. 179–84.
76. C.-Y. Hsu, T.-S. Sheu, J.-W. Yeh, and S.-K. Chen: *Wear*, 2010, vol. 268, pp. 653–59.
77. G.A. Salishchev, M.A. Tikhonovsky, D.G. Shaysultanov, N.D. Stepanov, A.V. Kuznetsov, I.V. Kolodiy, A.S. Tortika, and O.N. Senkov: *J. Alloy. Compd.*, 2014, vol. 591, pp. 11–21.
78. Z.Y. Rao, X. Wang, J. Zhu, X.H. Chen, L. Wang, J.J. Si, Y.D. Wu, and X.D. Hui: *Intermetallics*, 2016, vol. 77, pp. 23–33.
79. W.H. Liu, Z.P. Lu, J.Y. He, J.H. Luan, Z.J. Wang, B. Liu, Y. Liu, M.W. Chen, and C.T. Liu: *Acta Mater.*, 2016, vol. 116, pp. 332–42.
80. T.-T. Shun, L.-Y. Chang, and M.-H. Shiu: *Mater. Charact.*, 2012, vol. 70, pp. 63–67.
81. H. Jiang, H. Zhang, T. Huang, L. Yiping, T. Wang, and T. Li: *Mater. Des.*, 2016, vol. 109, pp. 539–46.
82. C.-C. Juan, K.-K. Tseng, W.-L. Hsu, M.-H. Tsai, C.-W. Tsai, C.-M. Lin, S.-K. Chen, S.-J. Lin, and J.-W. Yeh: *Mater. Lett.*, 2016, vol. 175, pp. 284–87.
83. J.M. Zhu, H.M. Fu, H.F. Zhang, A.M. Wang, H. Li, and Z.Q. Hu: *Mater. Sci. Eng., A*, 2010, vol. 527, pp. 6975–79.
84. X.C. Li, D. Dou, Z.Y. Zheng, and J.C. Li: *J. Mater. Eng. Perform.*, 2016, vol. 25, pp. 2164–69.
85. Y.D. Wu, Y.H. Cai, X.H. Chen, T. Wang, J.J. Si, L. Wang, Y.D. Wang, and X.D. Hui: *Mater. Des.*, 2015, vol. 83, pp. 651–60.
86. H. Jiang, L. Jiang, D. Qiao, Y. Lu, T. Wang, Z. Cao, and T. Li: *J. Mater. Sci. Technol.*, 2016, https://doi.org/10.1016/j.jmst.2016.09.016.
87. L. Jiang, L. Yiping, Y. Dong, T. Wang, Z. Cao, and T. Li: *Appl. Phys. A*, 2015, vol. 119, pp. 291–97.
88. C.-C. Juan, C.-Y. Hsu, C.-W. Tsai, W.-R. Wang, T.-S. Sheu, J.-W. Yeh, and S.-K. Chen: *Intermetallics*, 2013, vol. 32, pp. 401–07.
89. Y. Dong, D.X. Qiao, H.Z. Zhang, Y.P. Lu, T.M. Wang, and T.J. Li: *Mater. Sci. Forum*, 2016, vol. 849, pp. 40–44.
90. Z. Wang, W. Margaret, Z. Cai, S. Chen, and I. Baker: *Intermetallics*, 2016, vol. 75, pp. 79–87.
91. T.-T. Shun, L.-Y. Chang, and M.-H. Shiu: *Mater. Sci. Eng. A*, 2012, vol. 556, pp. 170–74.
92. H.W. Yao, J.W. Qiao, M.C. Gao, J.A. Hawk, S.G. Ma, H.F. Zhou, and Y. Zhang: *Mater. Sci. Eng., A*, 2016, vol. 674, pp. 203–11.

93. Z.D. Han, N. Chen, S.F. Zhao, L.W. Fan, G.N. Yang, Y. Shao, and K.F. Yao: *Intermetallics*, 2017, vol. 84, pp. 153–57.
94. Y.J. Zhou, Y. Zhang, Y.L. Wang, and G.L. Chen: *Appl. Phys. Lett.*, 2007, vol. 90, p. 181904.
95. Y. Dong, K. Zhou, L. Yiping, X. Gao, T. Wang, and T. Li: *Mater. Des.*, 2014, vol. 57, pp. 67–72.
96. N.D. Stepanov, D.G. Shaysultanov, G.A. Salishchev, M.A. Tikhonovsky, E.E. Oleynik, A.S. Tortika, and O.N. Senkov: *J. Alloy. Compd.*, 2015, vol. 628, pp. 170–85.
97. H. Jiang, L. Jiang, K. Han, L. Yiping, T. Wang, Z. Cao, and T. Li: *J. Mater. Eng. Perform.*, 2015, vol. 24, pp. 4594–4600.
98. R. Razuan: *Mater. Sci. Forum*, 2016, vol. 846, pp. 20–26.
99. X. Liu, W. Lei, L. Ma, J. Liu, J. Liu, and J. Cui: *J. Alloy. Compd.*, 2015, vol. 630, pp. 151–57.
100. N.N. Guo, L. Wang, L.S. Luo, X.Z. Li, R.R. Chen, Y.Q. Su, J.J. Guo, and H.Z. Fu: *J. Alloy. Compd.*, 2016, vol. 660, pp. 197–03.
101. J.M. Zhu, H.M. Fu, H.F. Zhang, A.M. Wang, H. Li, and Z.Q. Hu: *Mater. Sci. Eng., A*, 2010, vol. 527, pp. 7210–14.
102. N.N. Guo, L. Wang, L.S. Luo, X.Z. Li, R.R. Chen, Y.Q. Su, J.J. Guo, and H.Z. Fu: *Intermetallics*, 2016, vol. 69, pp. 74–77.
103. C. Li, B. Wang, Y. Zhang, C. Song, and Q. Zhai: *2nd Int. Conf. Adv. Energy, Environ. Chem. Eng.* 2016, pp. 10–15.
104. Z. Wang, I. Baker, W. Guo, and J.D. Poplawsky: *Acta Mater.*, 2017, vol. 126, pp. 346–60.
105. Z. Wu, C.M. Parish, and H. Bei: *J. Alloy. Compd.*, 2015, vol. 647, pp. 815–22.
106. F. Otto, A. Dlouhý, H. Ch Somsen, G.E. Bei, and E.P. George: *Acta Mater.*, 2013, vol. 61, pp. 5743–55.
107. N.D. Stepanov, N. Yu Yurchenko, M.A. Tikhonovsky, and G.A. Salishchev: *J. Alloy. Compd.*, 2016, vol. 687, pp. 59–71.
108. Y. Zhang, S.G. Ma, and J.W. Qiao: *Metall. Mater. Trans. A*, 2011, vol. 43, pp. 2625–30.
109. S.G. Ma, S.F. Zhang, J.W. Qiao, Z.H. Wang, M.C. Gao, Z.M. Jiao, H.J. Yang, and Y. Zhang: *Intermetallics*, 2014, vol. 54, pp. 104–109.
110. Y. Brif, M. Thomas, and I. Todd: *Scripta Mater.*, 2015, vol. 99, pp. 93–96.
111. R. Zhou, Y. Liu, C. Zhou, S. Li, W. Wu, M. Song, B. Liu, X. Liang, and P.K. Liaw: *Intermetallics*, 2018, vol. 94, pp. 165–71.
112. Z.G. Zhu, Q.B. Nguyen, F.L. Ng, X.H. An, X.Z. Liao, P.K. Liaw, S.M.L. Nai, and J. Wei: *Scripta Mater.*, 2018, vol. 154, pp. 20–24.
113. I. Kunce, M. Polanski, K. Karczewski, T. Plocinski, and K.J. Kurzydlowski: *J. Alloy. Compd.*, 2015, vol. 648, pp. 751–58.
114. T. Fujieda, H. Shiratori, K. Kuwabara, T. Kato, K. Yamanaka, Y. Koizumi, and A. Chiba: *Mater. Lett.*, 2015, vol. 159, pp. 12–15.
115. V. Ocelík, N. Janssen, S.N. Smith, J. Th, and M. De Hosson: *JOM*, 2016, vol. 68, pp. 1810–18.
116. C. Haase, F. Tang, M.B. Wilms, A. Weisheit, and B. Hallstedt: *Mater. Sci. Eng., A*, 2017, vol. 688, pp. 180–89.
117. S. Fang, W. Chen, and F. Zhiqiang: *Mater. Des.*, 2014, vol. 54, pp. 973–79.
118. S. Varalakshmi, G.A. Rao, M. Kamaraj, and B.S. Murty: *J. Mater. Sci.*, 2010, vol. 45, pp. 5158–63.
119. S. Varalakshmi, M. Kamaraj, and B.S. Murty: *Metall. Mater. Trans. A*, 2010, vol. 41A, pp. 2703–09.
120. W. Ji, F. Zhengyi, W. Wang, H. Wang, J. Zhang, Y. Wang, and F. Zhang: *J. Alloy. Compd.*, 2014, vol. 589, pp. 61–66.
121. C. Wang, W. Ji, and F. Zhengyi: *Adv. Powder Technol.*, 2014, vol. 25, pp. 1334–38.
122. Z. Chen, W. Chen, W. Bingyong, X. Cao, L. Liu, and F. Zhiqiang: *Mater. Sci. Eng. A*, 2015, vol. 648, pp. 217–24.
123. I. Moravcik, J. Cizek, J. Zapletal, Z. Kovacova, J. Vesely, P. Minarik, M. Kitzmantel, E. Neubauer, and I. Dlouhy: *Mater. Des.*, 2017, vol. 119, pp. 141–50.
124. A.J. Zaddach, C. Niu, C.C. Koch, and D.L. Irving: *JOM*, 2013, vol. 65, pp. 1780–89.
125. Y. Liu, J. Wang, Q. Fang, B. Liu, W. Yuan, and S. Chen: *Intermetallics*, 2016, vol. 68, pp. 16–22.
126. B. Cai, B. Liu, S. Kabra, Y. Wang, K. Yan, P.D. Lee, and Y. Liu: *Acta Mater.*, 2017, vol. 127, pp. 471–80.
127. Z. Fu, W. Chen, H. Xiao, L. Zhou, D. Zhu, and S. Yang: *Mater. Des.*, 2013, vol. 44, pp. 535–39.
128. S. Praveen, B.S. Murty, and R.S. Kottada: *JOM*, 2013, vol. 65, pp. 1797–1804.
129. Z. Fu, W. Chen, S. Fang, D. Zhang, H. Xiao, and D. Zhu: *J. Alloy. Compd.*, 2013, vol. 553, pp. 316–23.
130. W. Ji, W. Wang, H. Wang, J. Zhang, Y. Wang, F. Zhang, and F. Zhengyi: *Intermetallics*, 2015, vol. 56, pp. 24–27.
131. I. Moravcik, J. Cizek, P. Gavendova, S. Sheikh, S. Guo, and I. Dlouhy: *Mater. Lett.*, 2016, vol. 174, pp. 53–56.
132. Z. Tang, O.N. Senkov, C.M. Parish, C. Zhang, F. Zhang, L.J. Santodonato, G. Wang, G. Zhao, F. Yang, and P.K. Liaw: *Mater. Sci. Eng. A*, 2015, vol. 647, pp. 229–40.
133. J.S. Benjamin: *Metall. Trans.*, 1970, vol. 1, pp. 2943–51.
134. Z.A. Munir, U. Anselmi-Tamburini, and M. Ohyanagi: *J. Mater. Sci.*, 2006, vol. 41, pp. 763–77.
135. P. Wang, H. Cai, and X. Cheng: *J. Alloy. Compd.*, 2016, vol. 662, pp. 20–31.
136. P. Wang, H. Cai, S. Zhou, and X. Lingyu: *J. Alloy. Compd.*, 2017, vol. 695, pp. 462–75.
137. L. Rogal, D. Kalita, A. Tarasek, P. Bobrowski, and F. Czerwinski: *J. Alloy. Compd.*, 2017, vol. 708, pp. 344–52.
138. S. Varalakshmi, M. Kamaraj, and B.S. Murty: *Mater. Sci. Eng. A*, 2010, vol. 527, pp. 1027–30.
139. W. Chen, F. Zhiqiang, S. Fang, H. Xiao, and D. Zhu: *Mater. Des.*, 2013, vol. 51, pp. 854–60.
140. Z. Fu, W. Chen, H. Wen, Z. Chen, and E.J. Lavernia: *J. Alloy. Compd.*, 2015, vol. 646, pp. 175–82.
141. N. Eißmann, B. Klöden, T. Weißgärber, and B. Kieback: *Powder Metall.*, 2017, vol. 60, pp. 184–97.
142. X. Xian, Z. Zhong, B. Zhang, K. Song, C. Chen, S. Wang, J. Cheng, and W. Yucheng: *Mater. Des.*, 2017, vol. 121, pp. 229–36.